Cuadernos de Campo del Cuaternario, Nº 1

AEQUA Field-Guide Series, Vol. 1

C3

QTEC-AEQUA

2014

Tectonic geomorphology and paleoseismic records in the Eastern Betics Shear Zone and the Aguilas Arc (Murcia - Almería, SE Spain)

FIELD TRIP GUIDE IBERFAULT II – October 2014

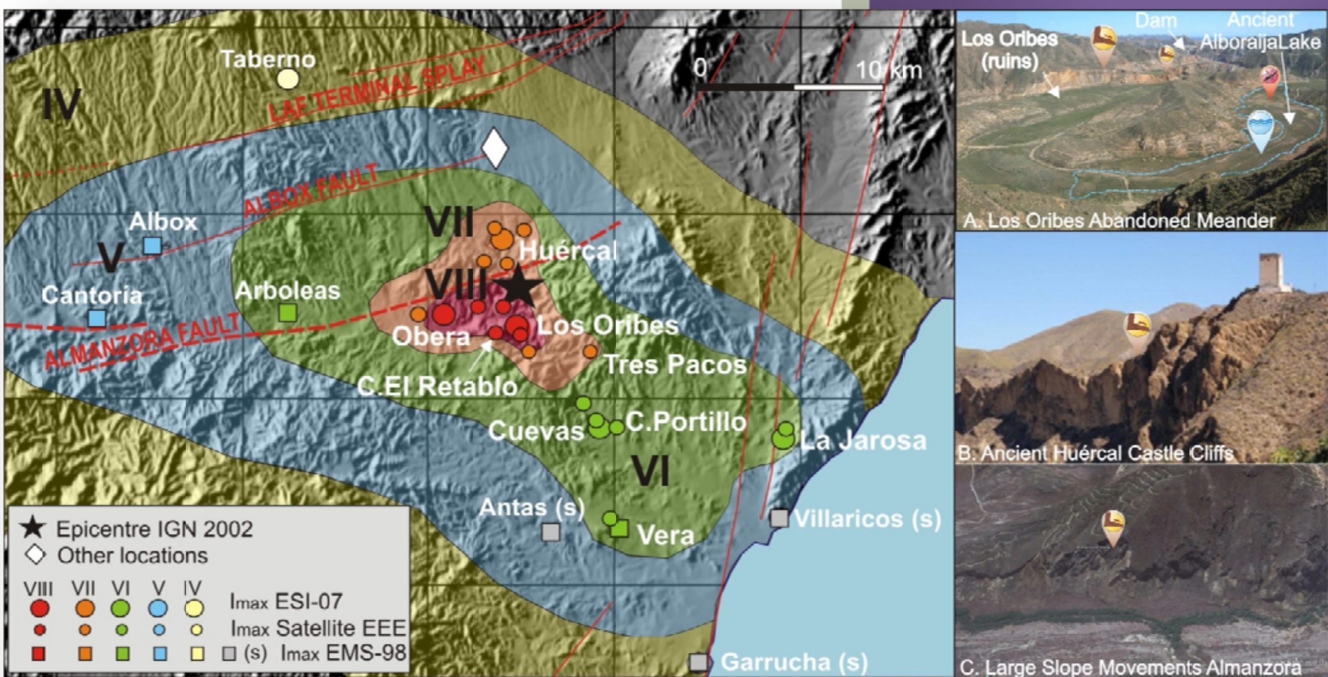

Pablo G. Silva (USAL)

Teresa Bardají (UAH)

Miguel A. Rodríguez-Pascua (IGME)

Elvira Roquero (UPM)

José J. Martínez Díaz (UCM)

GRUPO DE TRABAJO DE TECTÓNICA CUATERNARIA, PALEOSISMOLOGÍA y ARQUEOSISMOLOGÍA -AEQUA

ASOCIACIÓN ESPAÑOLA PARA EL ESTUDIO DEL CUATERNARIO - AEQUA

Publication supported by the MINECO research project CGL2012-37281-C02.01 (QTECTBETICA -USAL)

C^3

Cuadernos de Campo del Cuaternario

Guías de Campo de la Asociación Española para el Estudio del Cuaternario
AEQUA Field-Guide Series

ISSN-electrónico: **2386-8341**

Fotografía portada: Mapa Macrosísmico ESI-07 e ilustraciones de efectos geológicos cosísmicos más importantes correspondientes al terremoto de Huercál-Overa de 1863 AD (Silva et al., 2014).

Autor de la fotografía / imagen: Pablo G. Silva (Universidad de Salamanca)

Se recomienda citar las partes de esta obra de la siguiente forma:
Silva, P.G., Bardají, T. (2014). Rambla del Burruezo, Left-lateral drainage offsets and tectonic geomorphology of the Lorca – Alhama de Murcia fault zone. Murcia. En: Tectonic Geomorphology and paleoseismic records in the Eastern Betic Shear Zone and Aguilas Arc (Murcia - Almería, SE Spain). ***C^3 Cuadernos de Campo del Cuaternario***, 1. pp 7-8.

Edición y Maquetación:
Asociación Española para el Estudio del Cuaternario (AEQUA)
Escuela Politécnica Superior de Ávila (USAL).
Hornos Caleros, 50. 05003-Ávila, ESPAÑA
URL: www.aequa.es
e-mail: aequa@usal.es

Cuadernos de Campo del Cuaternario (C^3) es una **iniciativa editorial AEQUA** que pretende recopilar todas las actividades de campo ligadas a los grupos de trabajo de la asociación, así como a los congresos y reuniones científicas que esta organice o en las que colabore.

Editores de la Serie: Pablo G. Silva y Pedro Huerta (Departamento de Geología, Universidad de Salamanca)

Autores Vol. 1: Pablo G. Silva, Teresa Bardají, Miguel A. Rodríguez-Pascua, Elvira Roquero, José J. Martínez Díaz.

Título Vol. 1: *Tectonic Geomorphology and paleoseismic records in* Eastern Betic Shear Zone and Aguilas Arc *(Murcia - Almería, SE Spain). En Inglés.*

Congreso / Reunión: *Segunda Reunión sobre Falla Activas en la Península Ibérica. IBERFAULT II. Lorca (Murcia), 22-26 Octubre 2014.* ***Excursiones intra y post-congreso 24, 25 y 26 Octubre 2014.***

Agradecimientos / Acknowledgements Vol 1 (2014): *Work supported by the MINECO Spanish Research Projects CGL2012-37581-C02-01 (QTECTBETICA - USAL), CGL2012-33430 (CSIC), CGL2013-47412-C2-1-P (INTERGEO – UCM, CGL2013-42847-R (UNED) and ACI-2009-1037. This work is a contribution of the Spanish Working Group of the INQUA TERPRO Project 1299 (EEE Metrics), IGCP Project 588, INQUA CMP WG on Long Term Sea-level Changes and QTECT-AEQUA.*

INTRA and POST- CONGRESS FIELD TRIPS IBERFAULT II (QTECT- AEQUA). LORCA, MURCIA. OCTOBER, 2014

Tectonic Geomorphology and Paleoseismic records in the Eastern Betics Shear Zone and the Aguilas Arc (Murcia - Almeria, SE Spain)

Geomorfología Tectónica y Registros Paleosísmicos en la Zona de Cizalla de las Béticas Orientales y el Arco de Águilas (Murcia - Almería, SE España)

INDICE / INDEX.

C3

Cuadernos de Campo del Cuaternario

Vol 1 (2014). AEQUA

Tectonic Geomorphology and Paleoseismic records in the Eastern Betics Shear Zone and the Aguilas Arc

(Murcia - Almeria, SE Spain)

Edited by

P.G. Silva (USAL), T. Bardají (UAH), M.A. Rodríguez-Pascua (IGME) E. Roquero (UPM), J.J. Martínez Díaz (UCM),

Other Authors

A. Cabero (UNED). P. Carrasco-García (USAL), M. Ferrater (UB), Eulalia Masana (UB) M. Ortuño (UB), E. Rodríguez- Escudero (UAM)

Introduction and Itinerary

***P.G. Silva**. Dpt. Geology, University of Salamanca (USAL), Spain. pgsivla@usal.es*
***J. J. Martínez-Díaz**. Complutense University of Madrid, IGEO (UCM-CSIC) jmdiaz@ucm.es*

This field-trip is organized in the framework of the collaboration of the AEQUA Working Group on Quaternary Tectonics, Paleseismology and Archaeoseismology and IBERFAULT. Previous field-trips of QTECT-AEQUA were conducted in the Galera- Baza area (Granada; Garciá Tortosa et al, 2012) and in ancient Roman city of Baelo Claudia (Cádiz; Silva et al., 2013).

The field-trip is designed to illustrate the contribution of Quaternary Geology, Geomorphology and Structural Geology to the analysis of fault activity in the Eastern Betic Shear Zone and the Aguilas Arc, as well as to the macroseismic study of historical and recent earthquakes.

The first journey we will drive to the south of Lorca to have an overview of the relevant tectonic landscape developed along the southern segment of the Lorca—Alhama de Murcia fault zone (LAF). Driving to the south we will visit the E-W Almanzora Tectonic Corridor (ATC) to evaluate the contribution of earthquake environmental effects in the analysis of the AD 1863 Huércal-Overa and AD 1518 Vera earthquakes by means of the use of the ESI-07 macroseismic scale. Driving back to Lorca we will visit the Palomares fault in the vicinity of Puerto Lumbreras.

The second journey, we will start in the Castle of Lorca to see slope processes and archaeo-seismological damage triggered by the 2011 Lorca event. After that, we will take the Lorca-Águilas motorway, to visit nice exposures of bedrock fault scarps at the Tebar Castle zone. We will spent the rest of the day in the littoral zone of the Cope Basin (near Águilas) exploring synsedimentary deformations and height anomalies in marine terraces belonging to the Last interglacial (MIS 5) and uplifted Holocene

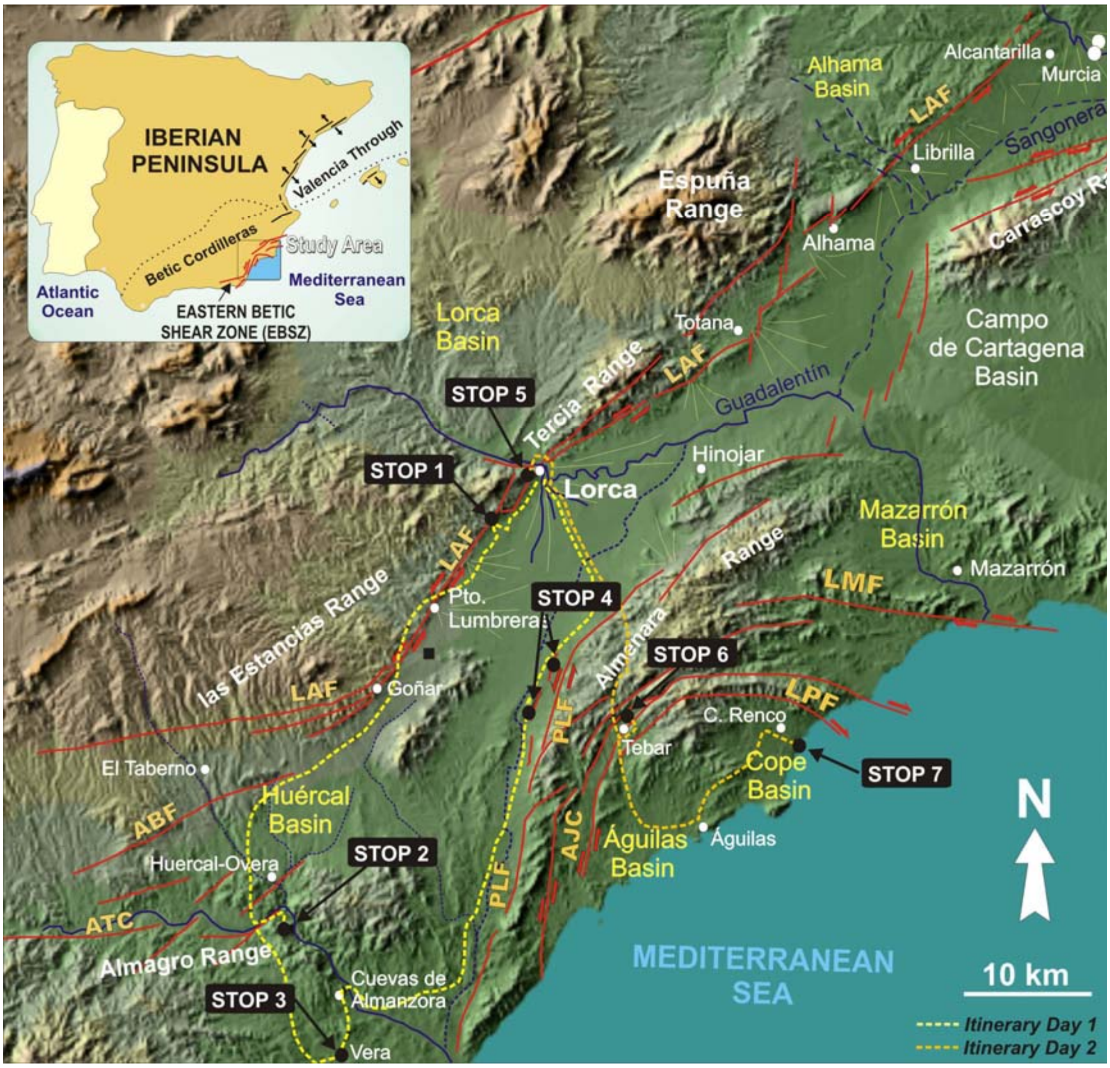

Fig. 0.1 Location Map and field-trip stops during days one and two. Legend: LAF: Lorca – Alhama de Murcia Fault; LMF: Las Moreras Fault; PLF: Palomares Fault; ABF: Albox Fault; ATC: Almanzora Tectonic Corridor; AJC: Los Arejos Tectonic Corridor.

marine platforms as a consequence of tectonic activity of the Águilas Arc.

The third journey contains the intra-congress short field-trip carried out during the Friday 24th October. This field-trip was specifically focused on the Alhama de Murcia fault in the vicinity of the locality of Lorca. The three field-outcrops provides a rapid outlook to the main structural, mechanical, geomorphlogical and paleoseismic evidences of two different fault segments around the urban zone of Lorca. Stop 8 (P1) was devoted to analyze the prominent fault-gouge outcropping at la rambla de La Torrecilla faulted mountain front area in the terminal zone of the southern segment of the AMF (Pto. Lumbreras – Lorca). In the second stop of this journey (P2; Stop 9) we moved to the most relevant central segment of the fault (Lorca – Totana) in the vicinity of the locality of La Hoya. At this place fault-branching generated a triangular strike-slip basin filled by alluvial fan deposits. Alluvial deposits have a nice geomorphological preservation and alluvial fan surfaces display outstanding evidence of surface faulting at mid-fan locations. Some of the alluvial fans overpassed the intervening tectonic reliefs generated by the fault allowing to explore relationships between sedimentation, tectonics and intersection point development. The third stop of the journey (P3; Stop 10) was located in a near place on the fault trace, where ongoing fault-trenching parallel and orthogonal to the fault provide stratigraphic and sedimentological evidence on left-lateral displacement of alluvial fan channels during the Late Pleistocene to the Holocene.

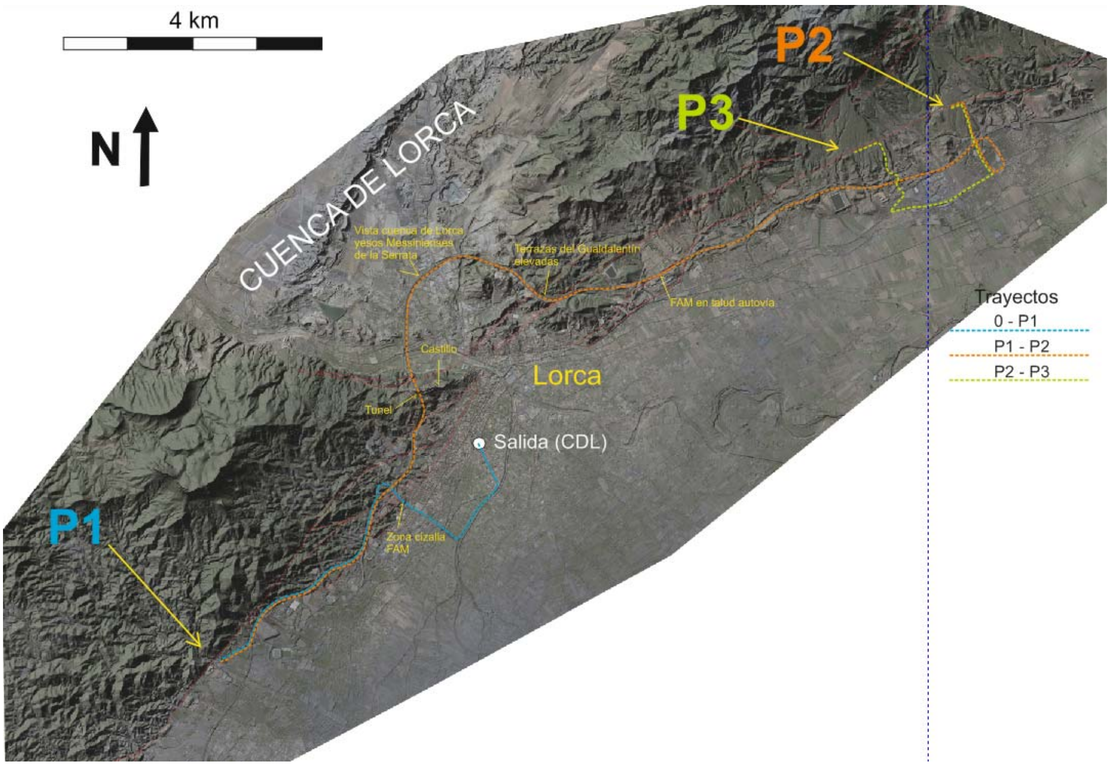

Fig. 0.2 Location Map and field-trip stops P1 (Stop 8), P2 (Stop 9) and P3 (Stop 3) during the third day of the field-trip (intra-congress field-trip IBERFAULT II)

Stop 1: Rambla del Burruezo. Left-lateral drainage offsets and tectonic geomorphology of the Lorca – Alhama de Murcia fault zone. Murcia

P.G. Silva. *Dpt. Geology, University of Salamanca (USAL), Spain. pgsilva@usal.es*
T. Bardají. *Dpt. Geology. University of Alcala de Henares (UAH), Spain. teresa.bardaji@uah.es*

This stop is situated about 3 km southwest of Lorca. It is located in the southern segment of the LAF and illustrates the tectonic geomorphology of a typical crustal-scale strike-slip fault zone (Fig.2.1). We have to walk up to the crest top beyond the offset channel of the rambla. In the far distance, looking to the north, you can see the Castle of Lorca and the nearby little watchtower of "La Torrecilla" (visited in the intra-congress field-trip). These landmarks outline the mountain front developed along this fault segment, as well as the more discrete set of spur (pressure) ridges adjacent to it. In fact we are standing on a little spur ridge of the fault some 80-100 m wide (Fig. 1.1). Looking now to the nearby rambla outcrop, we can see the internal structure of these spurs. High-angle reverse faulting overthrusted and pushed up the red Triassic beds and Alpujarrian phyllites over the Plio-Quaternary conglomerates (marginal fan systems). relatively undeformed fl akes of Tortonian conglomerates, Messinian(?) marls, and Precambrian/Cambrian schists are sandwiched. Now we have to retrace our steps back to the path along the crest of the spur ridge until its southern termination over the Rambla del Burruezo. Looking to the south, towards the industrial zone's water tower, four different ridge-hills spur between the present rambla valley (to the west) and the Guadalentín Depression (to the east). The rambla valley runs along the main fault zone, obvious from this point by the multicolored-banded landscape.

The aforementioned hills correspond to individual fan bodies made up of proximal conglomeratic lobes separated by finer distal sands and variegated clays. This present assemblage of sedimentary bodies is a primary consequence of the successive overlapping of fan lobes to the NE for about 1600 m, which

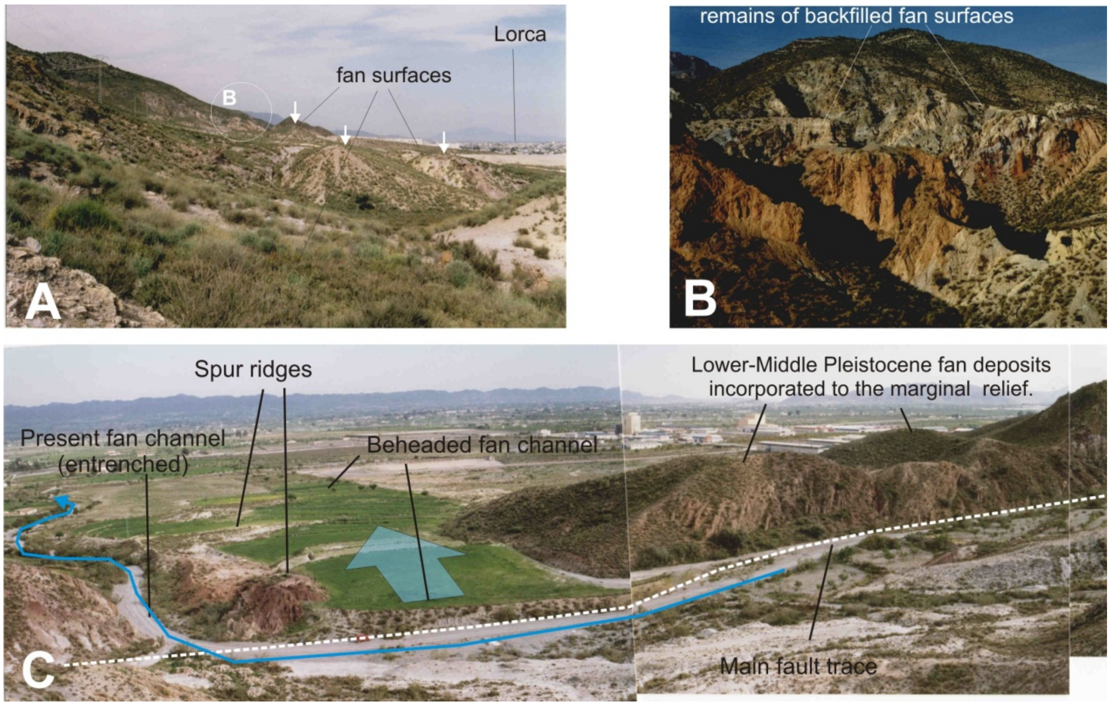

Fig. 1.1. A: Shutter ridges and spur-ridges developed along the LAF south of Lorca City (white arrows). Note the interference of the fault zone with the alluvial fan surfaces belonging to the second depositional phase (backfilling). B: View of the LAF Fault zone south of the Lorca City (location see fig 6A) with remains of the backfilled fan surfaces on the fault zone. C: Panoramic view of a left-lateral beheaded channel along the Pto.Lumbreras-Lorca Fault segment (LAF) south of the Lorca city. Note red car in the deflected channel bed for scale (Burruezo fan, location in Fig. 5). Photos P.G. Silva (1994).

Along the adjacent valley, to the left, runs the main fault zone, about 500 m wide in this sector. The fault zone is made up of a set of fault gouges of Alpujarride (schists and phyllites) and Malaguide (red-wine beds) among which indicates the dominant left lateral behavior of the LAF in this segment (Fig.1.3). Looking to the present rambla valley we can now observe the most recent impact of left-lateral kinematics on drainage development.

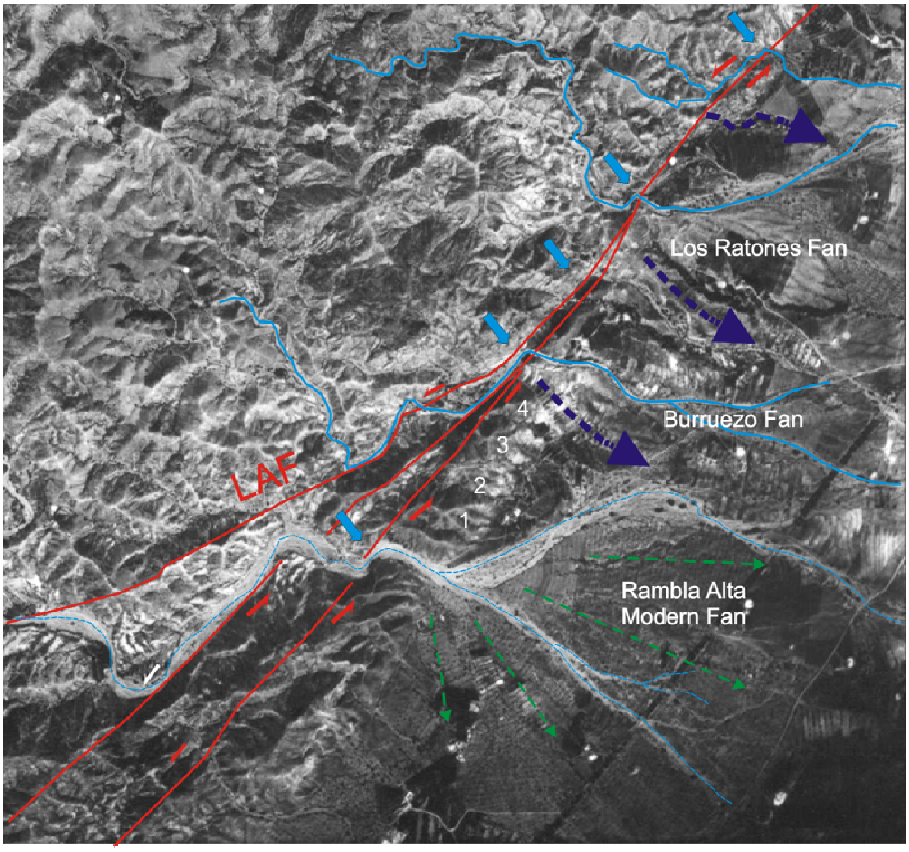

Fig. 1.2. Aerial Photograph (1:30.000) showing left-lateral channel offsets and deflections along the LAF south of the Lorca City. Note the Burruezo fan and behead channel illustrated in figure 2. Blue arrows indicate the major channel deflections and offsets with bayoneted-like pattern. Numbers (1 to 4) indicate the position of Lower-Middle Pleistocene old fan lobes incorporated to the marginal relief due to the activity of the fault.

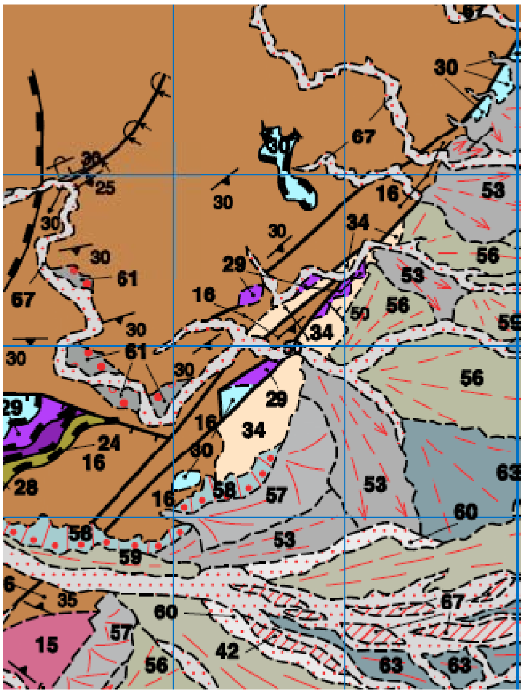

Fig. 1.3. (Left) Geological Map MAGNA 3rd Serie of the zone

The present rambla traces a prominent bayonet more than 250 m in length. Today it is possible to observe the actual offset channel (trenched) and the former beheaded channel (untrenched). Surveys of this zone indicate that channel offsets were a main characteristic of this particular sector of the LAF prior to the southern segment termination at the Lorca Contractional Duplex (LCD).

The more recent left-lateral displacement recorded by channel offsets range between ca. 50 to ca. 25 m, from south to north, suggesting a progressive buffering of displacements towards the LCD, where major earthquake nucleation takes place. Instrumental seismic records seem to indicate that aseismic creep operates in this fault segment accumulating tectonic stress over the LCD (a segment boundary) where major earthquakes are prone to occur.

Acknowledgements: *Work funded by the Spanish Research Project CGL2012-37581-C02-01 (QTECT BETICA - USAL) and INQUA TERPRO 1299.*

Stop 2: Cañón del Almanzora. Earthquake Environmental Effects triggered by the AD 1863 Huércal-Overa Earthquake, Almería (The Alboraija Lake)

P.G. Silva. *Dpt. Geology, University of Salamanca (USAL), Spain.* *pgsilva@usal.es*
E. Roquero. *Dpt. Pedology, Technical University of Madrid (UPM), Spain.* *elvira.roquero@upm.es*

On 10th June 1863 occurred the main event (M 4.2; VI-VII EMS / VII MSK) of the Huércal-Overa (Almería) seismic serie that extended till 23rd September of that year. The seismic serie included more than 40 aftershocks or related events, extended east (Huércal) to west (Serón) along the Almanzora Tectonic Corridor (ATC) and the southern localities of Cuevas de Almanzora and Vera (Espinar Moreno, 1994). Some of the aftershocks recorded EMS intensities of V-VI at Huércal and Serón, but also of IV-V at Cuevas, Vera and Huércal-Overa from July to September (Mártinez Solares and Mezcua,2002), inducing repeated environmental damage (De Prado, 1863).

This earthquake is interesting because produced an unusual large amount of earthquake environmental effects (EEEs) in spite of the moderate magnitude (M 4.2) and intensity (VI-VII EMS) assigned to the earthquake in the IGN catalogue (Mártinez Solares and Mezcua, 2002), previously of intensity VII MSK (Espinar Moreno, 1994). Epoch field data by De Prado (1863), historical data reported by Madoz (1845), Garcia Asensio (1908) and news from epoch journals (Fernández Bolea, 2009) let to identify and locate most of the documented EEEs (Silva et al., 2014). The analysis of these data let to recognize the occurrence of hydrologic and hydrogeologic anomalies, ground cracks, slope movements, anomalies in water bodies (river and small lakes) and several secondary effects such as, tree shacking, gas emissions and spontaneous ventilation of underground mines.

A total of 21 EEE records are available for this earthquake (Silva et al., 2014; Fig.2.1). Most of them are considered in the ESI-07 Scale (Michetti et al., 2007) being possible to develop a detailed macroseismic analysis. This preliminary analysis points to the occurrence of EEEs VIII ESI within the Almanzora Canyon-Valley, 4-5 km south of Huércal-Overa, no considered or properly identified in previous analyses.

Earthquake environmental effects produced by the AD 1863 Huércal-Overa event corresponds to secondary effects of the ESI-07 Scale. The main ones are included in the category of slope movements, mainly as large to moderate rockfalls. Multiple ground cracks occurred in the localities of Huércal-Overa, Cuevas de Almanzora, Los Oribes and the ancient Obera (Fig. 2.1). The two last localities, about 3 to 4.5 km away from the epicenter, record relevant anomalies on water bodies indicating an intensity VIII ESI-07 over an area of c. 10 km^2 (Fig. 2.2). It is noteworthy that the original report of De Prado (1863) clearly indicates that the most damaged area both, during the main event and the subsequent seismic serie was the zone of the ancient locality of Obera, within the

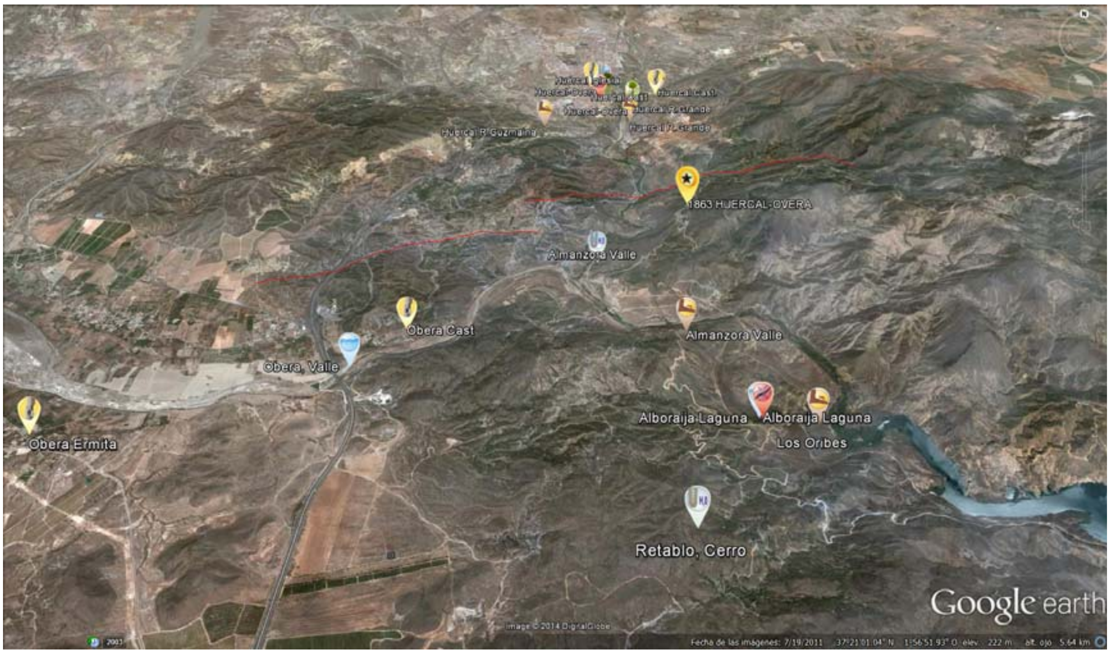

Fig. 2.1. A: Google earth image showing the distribution of Earthquake environmental effects related to the AD 1863 Huércal-Overa Earthquake. Environmental damage identified within the Almanzora Canyon-valley around the ancient sites of Obera and Los Oribes indicate the occurrence of a zone of intensity VIII ESI-07

Almanzora valley, nearly depopulated in the epoch (ref. *"Despoblado de Obera"*).

In the macroseismic area, the Almanzora river stopped or diminished its flow-rate inducing that some watermills stopped working during some minutes in the ancient Obera zone. In Los Oribes an ancient small lake basin (Laguna de Alboraija) disappeared as a consequence of the formation of large ground cracks in its floor. The disappeared lake (30,000 m^2 and 4-5 m depth) was located in an incised abandoned meander belonging to the T+20m fluvial terrace of the Almanzora river (Stokes and Mather, 2003). The emptied lake floor displayed an irregular cracked topography being impossible its survey for almost a year, when ground-cracks were filled by alluvial deposits derived from strong rain-fall events (De Prado, 1863; Fig. 2.3). Taking into account the dimensions of the lake and the emptied volume of water (c. 150,000 m^3) ground cracks were probably hectometric in length and metric in width. This emptied lake is again functional as a consequence of the construction of the Almanzora dam in the early 90`s, a few kilometers downstream. These two processes (abrupt decrease of flow-rates and emptied water bodies) are considered in the ESI-07 scale from intensities ≥ VIII (Michetti et al., 2007).

Additionally some hydrogeological anomalies in springs occurred in the area indicating intensity VIII-ESI-07. One spring within the Almanzora river run dry during 15 days and moved 40 m after the event to a different elevation causing the new spring the death of the surrounding vegetation (De Prado, 1863). Field-survey and historical data reported by Madoz (1845) led to identify this spring with "La Fuente de Obera" located in the ancient sanctuary of "La Santa" 1.2 km away from the epicenter, at the Bobara-Almanzora rambla-junction. Data from García Asensio (1908) stated that in the whole Sierra the Almagro was common the occurrence of new upwelling sulphorous muddy water-springs, but especially around hill of El Retablo, 0.8 km west from Los Oribes (Fig. 2.1).

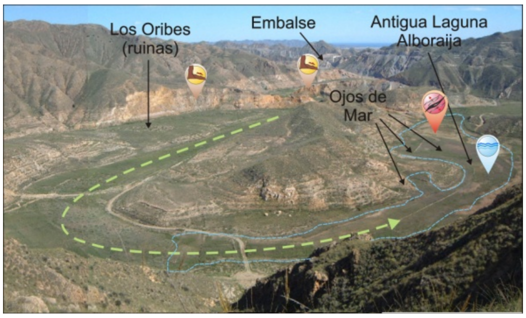

Fig. 2.3. View of the abandoned incised meander of Los Oribes, where was placed the Alboraija Lake emptied during the AD 1863 Huércal-Overa event.

Also in this sector of the Almanzora canyon large rockfalls were produced as reported by De Prado (1863) and Fernández Bolea (2009). Silva et al. (2014) identifies eleven zones, where large rock-falls are common within the valley, but only consider six ones for the macroseismic analysis. The larger ones display landslide scars up to 100 m length and individual mobilized volumes >50,000 m^3 (Fig. 2.2).

The macroseismic analysis of EEEs triggered by the Huércal-Overa earthquake, expand the number of information points, improving previous analyses only based in building damage. The results obtained for Silva et al. (2014), record damage of intensity VIII within the Almanzora valley, depopulated in the epoch of the earthquake and multiplies intensity data around the locality of Huercal-Overa and Cuevas de Almanzora (Fig. 2.2) leading to a more detailed delineation of intensity zones than previous studies based on EMS data for only 6 localities.

Acknowledgements: *Work funded by the Spanish Research Project CGL2012-37581-C02-01 (QTECT BETICA - USAL) and INQUA TERPRO 1299.*

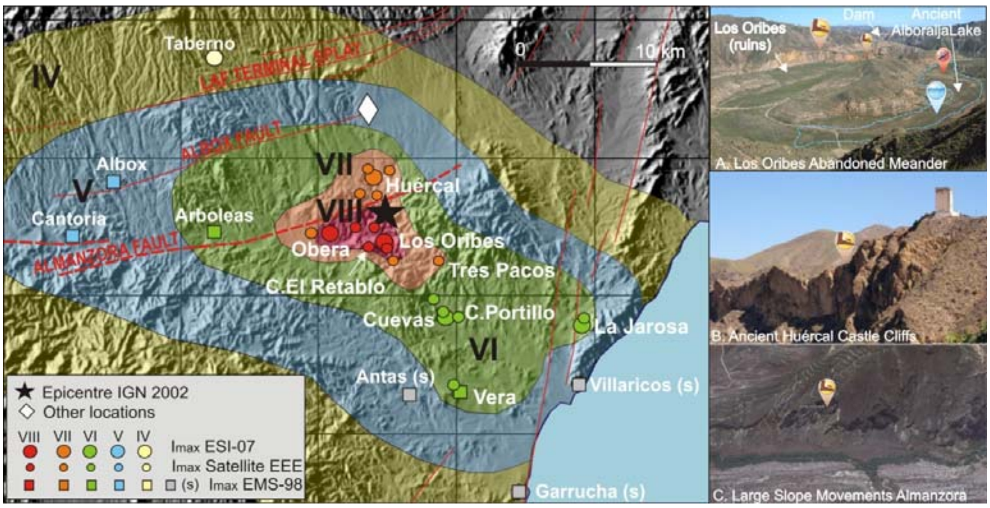

Fig. 2.2. Map of Intensity zones of the AD 1863 Huércal-Overa Earthquake deduced from Environmental damage ESI-07 data and building-damage EMS-98 data. Red lines: main faults of the zone. To the left images of selected EEEs described in the text

Stop 3: Cerro del Espiritu Santo: Earthquake Environmental Effects triggered by the AD 1518 Vera Earthquake (Almería).

***P.G. Silva**. Dpt. Geology, University of Salamanca (USAL), Spain. pgsilva@usal.es*
***E. Roquero.** Dpt. Pedology, Technical University of Madrid (UPM), Spain. elvira.roquero@upm.es*

In November 9th AD 1518 two closely spaced earthquakes occurred in the old city of Vera. Estimated maximum intensity was VIII-IX EMS (Martínez Solares and Mezcua, 2002), previously in the range of X MSK (Espinar Moreno, 1994). In spite of these intensity estimations the two earthquakes caused the total destruction of the Castle (Alcazaba), city walls and the collapse of all edifices of the village (about 200 houses). The earthquake caused 150 casualties and many injured people. Only the "Santísimo" Chapel (old mosque) and a cistern were no totally destroyed. (IGN, 1995).
The city had to be moved from its ancient place (Cerro del Espíritu Santo) and rebuilt in its present place down to the hill.

Macroseismic data are only available for two more localities, Mojacar (12 km away) and the little fishing village of Garrucha (6 km away). In Mojácar (VIII EMS;) virtually collapsed most of the towers and large sectors of the city wall. A third of the houses destroyed (about 20 houses), leaving the rest uninhabitable; 15 casualties and many injuries. Moderate damage occurred in Garrucha (VI-VII EMS), and in Cuevas de Almazora, where the earthquake was felt, but no data are available on possible damage, it is only documented that the population left the village as a consequence of the damage in houses, but some historical data indicate that in this village the damage was not less than in Vera (IGN, 1995).

Although, only three intensity points are available for this event, some authors (Vincent, 1989) generated an MSK intensity map for the event implicitly relating the earthquake with the trace of the well-known Palomares strike-slip fault (Espinar Moreno, 1994). This last author, and many others, think that the intensity map is not of use, because the scarce number of intensity points (IGN, 1995).

Historical data collected by IGN (1995) and recent field-survey (Silva, 2014) clearly indicate that environmental damage by secondary effects is only documented for the old place of Vera (macroseismic epicentre), located in the Cerro del Espíritu Santo (Hill). This is a structural butte on subhorizontal conglomerates, sandstones (top) and marls (base) of Pliocene age, which collapsed entirely triggering relevant large rockfalls damaging the downslope sector of the city. Large ground crack and rockfall processes triggered large-scale ground failures in the foundations of the ancient Arab Castle placed in the top of the hill. As a consequence of the earthquake one of the main springs of the village dried up (IGN, 1995)

Large rockfalls, with individual blocks of 50 to 350 m^3, occurred in the Cerro del Espiritu Santo. Fallen blocks occur in every orientation around the hill, but mainly affecting their northern, north-eastern and southern slopes. The last one develop a near-vertical cliff. Whatever the case largest blocks did not fallen downslope and presently they display and apparent radial disposition around the top of the butte. The original perimeter of the top of the butte is estimated in 130 m, but at present only 80 to 90 m remains, and consequently about the 35% of the ancient butte surface collapsed during the earthquake. Rocky blocks of even 100 m^3 rolled downslope with run-outs of about 120 to 180 m.

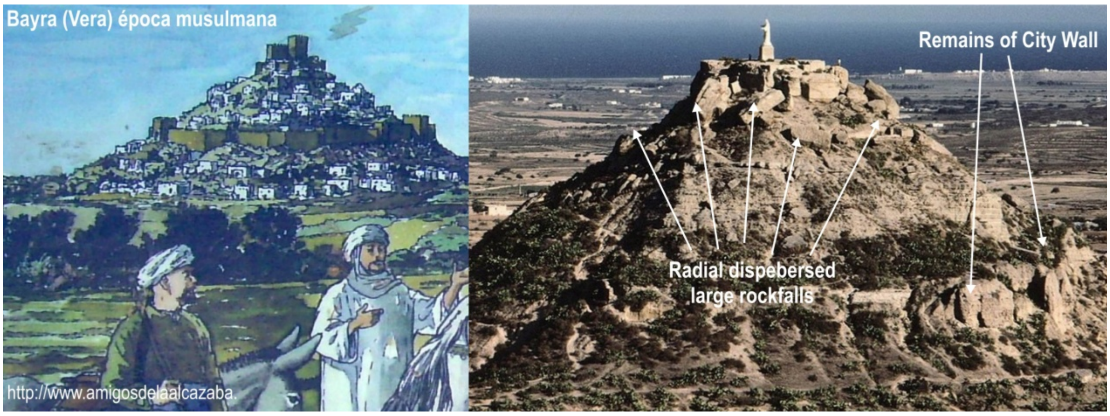

Fig. 3.1. Pictorial recreation of the old Vera (Bayra) during the Muslim period with the Alcazaba (castle) crowning the city before its destruction (Association of Friends of La Alcazaba of Almeria). Current view (from the south) of the Holy Spirit Cerro showing landslides and debris block walls (Photo Helios: verapueblo / blogspot.org)

Fig. 3.2. View of the Cerro del Portillo in the environs of Cuevas de Almanzora showing similar level of damage by slope processes than in the Vera case (Silva et al., 2014).

Rock-falls were generated as a consequence of the development of large coseismic open cracks in the rocky materials topping structural. As still can be observed today, open fractures in the rock are 20-30 cm wide, and in many cases display depths of 4-5 m. These display preferred N-S and E-W general orientations, facilitating the cracking and detachment of the rocky blocks. This description refers to no-detached blocks presently outcropping at the top of the butte, so rock cracks related with the really detached ones will extend over the nearly complete thickness of the conglomerate strata topping the butte (about 8 m thick).

Detached rocky blocks and remains of the city walls are scattered all around the hill slopes of the butte. It is no possible to establish any preferred orientation for ground sacking, except the record the overall amplified vibration of the hill increasing to the top, where fallen blocks are radially dispersed by topographic amplificationof ground shaking (Figs. 3.1 and 3.3).

As abovementioned there is few data for other localities In Mojácar, about 12 km SW of Vera and also founded on a hill, slope processes could also participate in the reported destruction of city walls and towers (in study). In Cuevas de Almanzora, 5.5 km NE from Vera, there are not historical documents illustrating the occurrence of similar slope movements, but most of the structural buttes (similar to the Espíritu Santo one) in the vicinity of Cuevas and between this locality and Vera, over a radius of 6 km (c. 110 km^2), display a similar level of destruction, with nearly complete collapses of the rocky strata topping them an indicating a minimum intensity ≥ VIII EMS (Silva et al., 2014) In detail, the analysis of the earthquake effects of the AD 1863 Huercal-Overa earthquake in Cuevas de Almanzora, the descriptions of García Asensio (1908) y Fernández Bolea (2009) indicate the occurrence on multiple rockfalls in the surrounding buttes (Fig. 3.2; Silva et al., 2014). Analyses of these coseismic effects identified several structural buttes (i.e. Cerro de El Portillo) displaying a similar level of destruction than in the case of Vera. Since intensity levels in Cuevas during the AD 1863 event only reached VI EMS, the main episode of butte destruction is assigned to the previous AD 1518 Vera event, indicating a minimum intensity of VIII ESI-07 (Silva et al., 2014).

Acknowledgements: Work *funded by the Spanish Research Project CGL2012-37581-C02-01 (QTECTBETICA - USAL). This work is a contribution of the Spanish Working Group of the INQUA TERPRO Project 1299 (EEE Metrics).*

Fig. 3.3. Early 20th century historical photography of the Cerro del Espiritu Santo (Old Vera) before its restoration in the 1970 decade. View from the SE. Note the large number of detached fallen blocks downslope. (Photo Helios: verapueblo/ blogspot.org)

Stop 4: La Escarihuela. Pleistocene faulted soil sequences in the Palomares Fault and Tectonic Geomorphology of the Fault Zone, Murcia

P.G. Silva. *Dpt. Geology, University of Salamanca (USAL), Spain.* *pgsilva@usal.es*
E. Roquero. *Dpt. Pedology, Technical University of Madrid (UPM), Spain.* *elvira.roquero@upm.es*
M.A. Rodríguez-Pascua. *Instituto Geológico y Minero de España (IGME).* *marodriguez@igme.es*
T. Bardají. *Dpt. Geology. University of Alcala de Henares (UAH), Spain.* *teresa.bardaji@uah.es*
P. Carrasco-García. *Dpt. Ingeniería del Terreno (USAL), Spain.* *pcarrasco@usal.es*

Natural fault exposures and fault-trench analysis are devoted to unravel the paleoseismic history of surveyed faults by means of the identification of discrete earthquake event horizons. We use offset paleosols as earthquake horizon events and soil development as a relative timing-clock tool in the natural exposures of the strike-slip Palomares Fault (PLF) located in the Murcia Region (Silva et al., 1997).

In this region paleoseismic studies indicate that stronger events have long recurrence between 15 and 30 ka, and maximum estimated magnitudes of 6.4 Mw to 7.0 Mw. This is mainly due to the slow fault slip rates (<0.5 m/ka) linked to the Africa-Eurasia plate convergence rates (4 mm/year) controlling the Quaternary tectonic activity in the Betic Cordillera (e.g. Martínez-Díaz et al., 2012).

Soils and faulting events at La Escarihuela outcrop.

The section studied is located in the locality of La Escarihuela, on the PLF fault trace. The section record a total amount of six paleosols on alluvial-colluvial deposits vertically displaced by the fault a maximum of 33 cm. The faulted soil sequence is sealed by an undisturbed thick (0.6 m) mature calcrete horizon at top. The paleosol

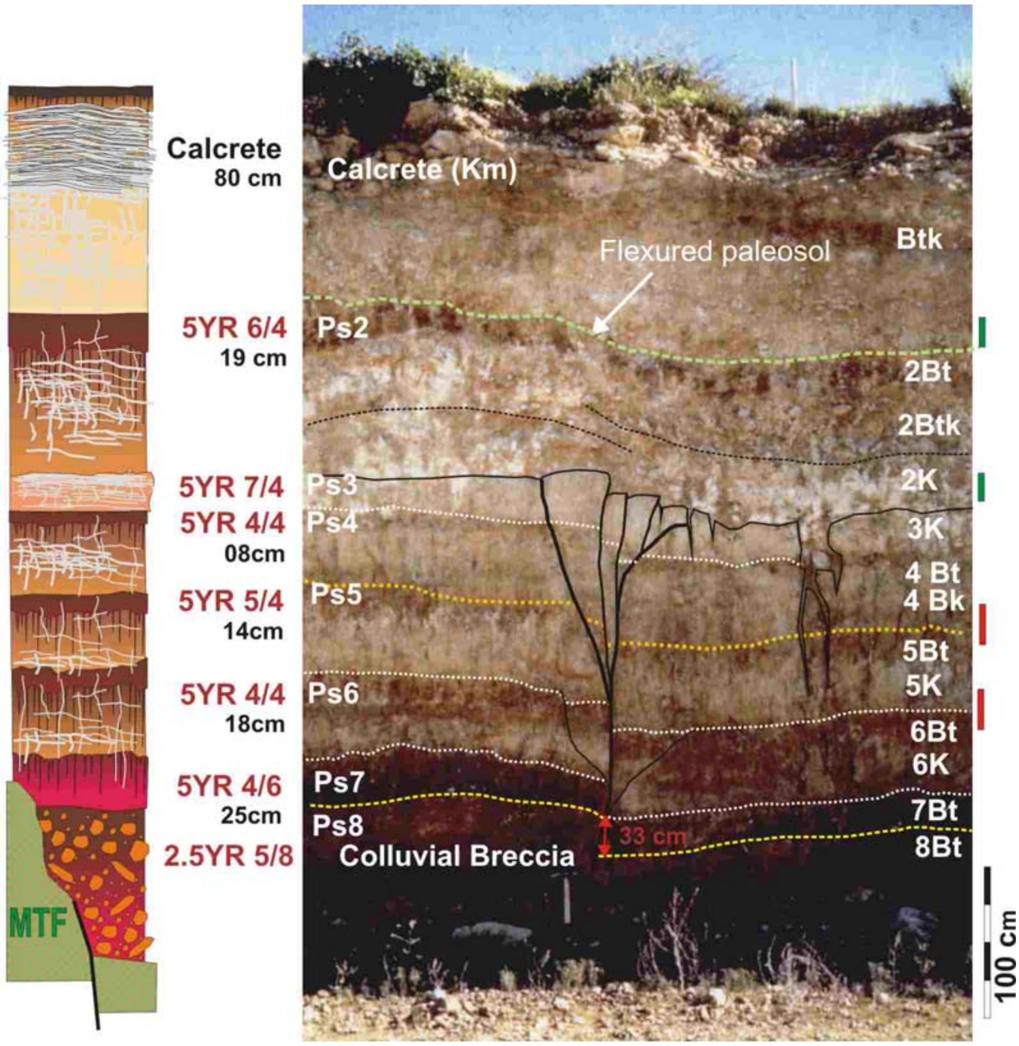

Fig.4.1. Diagrams, photos and maps illustrating repeated surface faulting along the Palomares fault from the analysis of soil sequences in La Escarihuela Site and fault scarps related with the linear tectonic relief of Cabezo del Muro at el Aljibejo site.

sequence develops on successive and overlapped sedimentary units, 50 to 20 cm thick, indicating alternating stages of soil formation and sedimentation evolving upwards to more arid conditions. This is evidenced by the increasing accumulation of carbonate on the original Bt horizons, leading the superposition of different pedogenetic cycles responsible of the recalcification of the underlying paleosols. The common horizon sequences are featured by reddish brown Bt horizons (5YR5/4d, 5YR4/4m) overlying calcic horizons ($CaCO_3$. 35%). In some cases these calcic horizons are originated by the recalcification of the existing Bt horizons giving place to a lightening (5YR 6/3d, 5/4m) associated with $CaCO_3$ content about 8-12%. Clay content are variable but soil colours are similar since they are mainly inherited from previous well developed red soils (2,5YR 4/6d, 3/6m) in the metamorphic source area. Recent dating of alluvial fan surfaces in the region, indicate that thick mature calcretes on alluvial sediments hold a minimum OSL ages of c. 330 ka BP (Ortuño et al., 2012).

Comparing soil features (e.g. soil depth/spacing, soil thickness, Bt thickness, clay and carbonate content) with the conventional Marine Oxygen Isotopic (MIS) curve is possible to establish preliminary relative paleoclimatic relationships and obtain a relative time-scale for soil development. Considering an age of c. 330 ka BP for the top calcrete horizon the complete sequence of paleosols developed between c. 612 ka BP (MIS 15) and c.337 ka BP (MIS 9), with peaks of soil formation during intervening warmer isotopic stages MIS 13 and 11. Comparing the obtained soil-time data and accumulated fault offsets (33 and 12 cm) is possible to discriminate two paleoseismic events with and vertical displacement per event of 21 cm (Event 1) and 12 cm (Event 2).

The Event 1 affects the three basal soils recording true surface faulting, but Event 2 only triggered surface flexure, both of reverse – strike-slip nature, with a recurrence period of c. 125 ka and estimated magnitudes of c. 5.9 Mw ± 0.2 and 6.4 Mw ± 0.3 respectively.

Paleosols provide a unique evidence of surface faulting in paleoseismology, since these particular geological elements can be unequivocally related to an ancient ground surface. In Mediterranean zones subject to slow convergence rates, the comparison of Middle-Late Pleistocene alluvial paleosol sequences with existing paleoclimatic time-scales can offer god approaches to establish the timing for the seismic history of a zone.

Tectonic geomorphology and related surface faulting events.

The Palomares fault in the Murcia region is bounding the eastern margin of the Guadalentín Depression south of Lorca, constituting the Almenara Mountain Front about 12 km east of the Las Estancias range-front fault controlled by the LAF (Silva et al., 1992; 2003). In this sector the PLF fault zone is 29 km long and 2 km wide displaying two main fault traces stepping the Almenara front piedmont and generating particular horst and graben topographies with metric offsets (Fig. 4.2; Silva et al., 1997; Silva and Bardají, 2013). In fact in this zone these two main fault strands generate linear surface faulting of consistent N010-020 orientation and normal fault kinematics, which contrast with the dominant and outstanding left-lateral strike slip deformations displayed by the PLF further to the south in the Almería region (Bousquet et al., 1975; Silva et al., 2003).

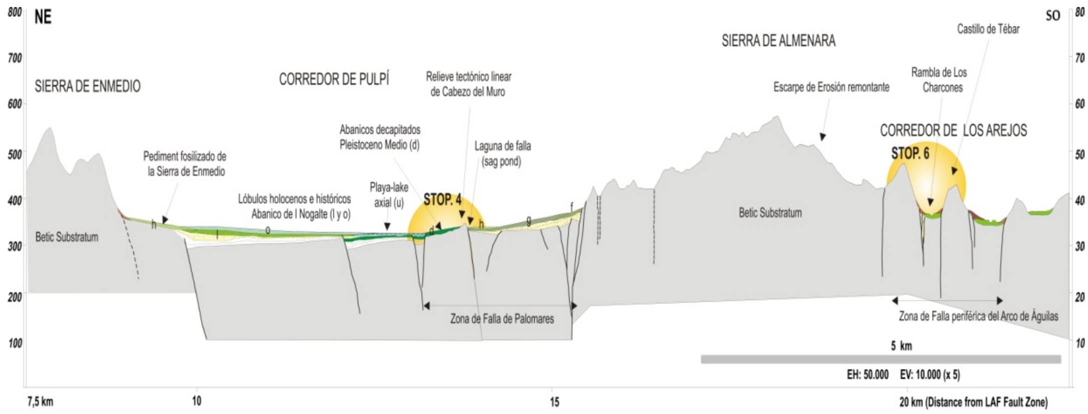

Fig. 4.2. Geomorphological cross-section illustrating main features of the subsiding tectonic corridors of Pulpi (East) and Los Arejos (West) and intervening tectonic reliefs. Location of stops 4 (La Escarihuela) and 6 (Tebar Castle) is highlighted. The Palomares and Los Arejos fault zones are the major shear zones bounding the Aguilas Arc (Tectonic Indenter active since Early Miocene times). Cross-section modified from Silva and Bardaji (2013).

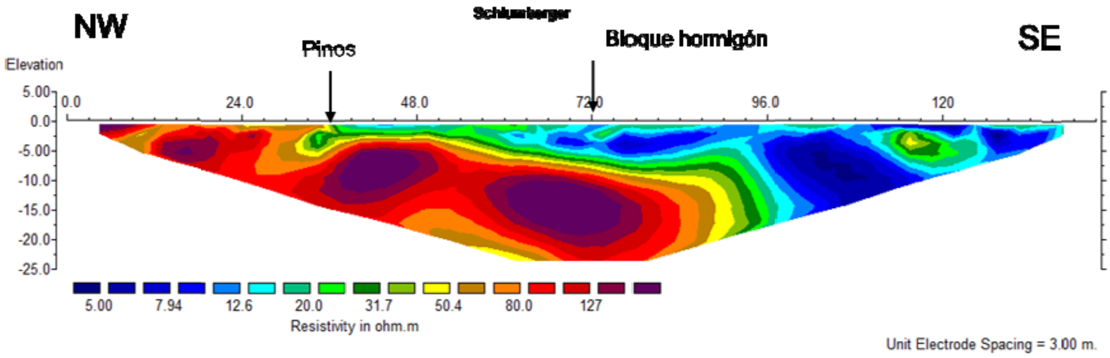

Fig. 4.3. Electrical tomography pseudosection of the Palomares Fault Zone at the Aljibejo Site. 142 m Schlumberger array.

At the Aljibejo zone, located 12 km east of Pto.Lumbreras (Aguilas-Pto.Lumbreras Route), Quaternary offsets are visible as very degraded normal fault scarps along the N012 main fault trace, which display a maximum rupture length of 12.8 km from the Locality of Pulpí (south) to the Aljibejo zone (north) distributed in small "en echelon" segments 3.8 to 2.3 km long. In most of the cases these scarps are totally buried by a colluvial wedge which contributes to the gentle slope of the present topographic step and indicate the old age of the surface rupture features (Fig. 4.1). These east-facing fault scarps cut-off Middle (ABJ1) to Late Pleistocene (ABJ2) fan surfaces, which show a mature and weak calcrete development, respectively of massive petrocalcic horizons 1.2 (ABJ1) to 0.6 m thick (ABJ2). Recent dating of fan surfaces in the zone of Goñar, about 15 km SW in the LAF Mountain front (Shobatti et al., 2011; Ortuño et al., 2012), allow to establish relationships between age and existing models of calcrete development for the zone (Alonso-Zarza et al., 1999).

These relationships (Silva, 2013) indicate that mature calcretes of el Aljibejo 1 site holds a minimum age of 330 ka BP (Middle Pleistocene), and therefore comparable to the calcrete developed on the top of the soil faulted sequence at La Escarihuela ocutcrop. On the other hand, cemented fan surfaces of el Aljibejo 2 site are less developed displaying only massive ck horizons, and can be considered to be formed during the onset of the Late Pleistocene (MIS 5), c. 110 ka BP (Silva, 2013). Fan surface maximum vertical offsets are of 2.5 m in el Aljibejo 1 site and of 1.8 m in el Aljibejo 2 site (Silva et al., 1997), but mean values are of 2.1 and 1.1 m respectively. The relative topographic dislocation promoted by surface faulting resulted in the impoundment (shuttering) of the drainage coming from the neighbouring Almenara range, triggering the development of small Holocene sag-ponds at the fault toe (Fig. 4.4). Surface rupture length affecting both sites is estimated in 5.3 km, taking into account its southern prolongation along the intrabasinal relief of Cabezo del Muro. This is a basement-involved linear tectonic relief bounded by a set of three staircased bedrock fault scarps ranging from 0.7 to 0.4 m high (Fig. 4), in which purely vertical fault plane striae are exposed, indicating a east-facing normal kinematics congruent with the morphology of the fault scarps (Silva et al., 1997).

Several 2D Electric Tomography pseudosections have been done along the Palomares Fault Zone in order to undertake further fault trenching. The obtained preliminary results indicate strong karstification of Betic substratum and apparent faulting on bedrock fault scraps presently buried by the most recent playa –lake sediments in the Aljibejo area (Fig. 4.3).

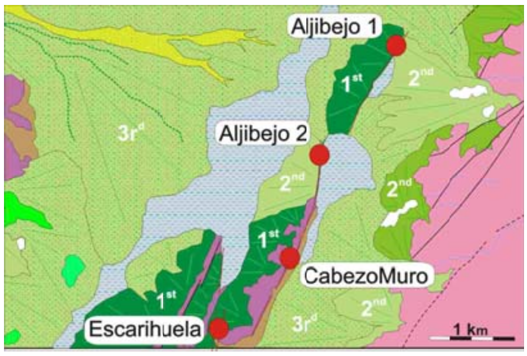

Fig. 4.4. Geomorphological Sketch-Map of alluvial fan systems in the Palomares Fault Zone in the studied area.

Acknowledgements: *Work funded by the Spanish Research Projects CGL2012-37581-C02-01 (QTECTBETICA - USAL), CGL2012-33430 (CSIC). This work is a contribution of the Spanish Working Group of the INQUA TERPRO Project 1299 (EEE Metrics).*

Stop 5: Lorca Castle. Rockfalls and Archaeoseismological Effects triggered by the 2011 5.1 Mw Earthquake. Murcia.

M.A. Rodríguez-Pascua. *Instituto Geológico y Minero de España (IGME). marodriguez@igme.es*
P.G. Silva*. Dpt. Geology, University of Salamanca (USAL), Spain. pgsilva@usal.es*

Lorca Castle is a fortress of medieval origin built between the 9th and 15th centuries. It consists of a series of defensive structures that, during the Middle Ages, made the town and the fortress an unconquerable point in the southeast part of the Iberian Peninsula. Lorca Castle was a key strategic point of contention between Christians and Muslims during the “Reconquista”.

Fig. 5.1.Google Earth aerial view of the Castle of Lorca. The symbols marc the location of the main rockfalls and the Eearquake Archaeological Effects (EAEs) generated by the Lorca Earthquake (2011/05/11).

The Lorca Castle is located in the top of a hill above the old sector of the town of Lorca. The hill corresponds to the series of structural reliefs developed on Tortonian limestone along the southern border of the Lorca Neogene Basin. All these structural reliefs (cuestas and buttes) suffered significant environmental damage during the May 11th Lorca earthquake (Alfaro et al., 2012; Silva et al., 2014). Most of the damage was in the form of rock falls, the IGME preliminary report on the earthquake (IGME, 2011) recorded more than 9 rock falls around the structural butte of the Castle, some of them also affecting to the defensive walls and watch towers(Fig. 5.1). Most of the research after the earthquake indicate that the topographic effect on the hill amplified the seismic waves triggering secondary coseismic rock falls.

The most important rock falls where recorded in the northern slope of the hill, whereas in the southern slope only minor slope processes occurred since it was already protected with “steel dynamic nets” preventing or mitigating the coseismic slope processes.

The most significant rockfall was recorded in the Eastern end (Espolón Este) of the defensive wall (Figs. 5.1; 5.2). The direction of collapse of this rockfall was N045ºE and affected to a maximum rock volume of about 100 m3. Some of the detached rock blocks had dimensions of 10 to 20 m3 and maximum run-outs of about 60 m. the defensive wall of the castle. However, some of the blocks dispersed to the ESE rolled down about 100 m causing damage in adjacent buildings (Fig. IGME, 2011).

Fig. 5.2.Main rockfall generated by the earthquake (2011/05/11) in the Castle of Lorca. Located in the NE part of the defensive wall.

Fig. 5.3: Damage produced in the wall of concrete blocks of a building triggered by a rock fall from the Eastern Espolón of the Castle.

The earthquake archaeoseismological effects (EAEs) (Rodríguez-Pascua et al., 2011) generated in the castle were mainly: collapsed walls, penetrative fractures and displaced masonry blocks (IGME, 2011). collapses affected to the defensive wall, mainly in the NW part of the wall (Fig. 5.1).

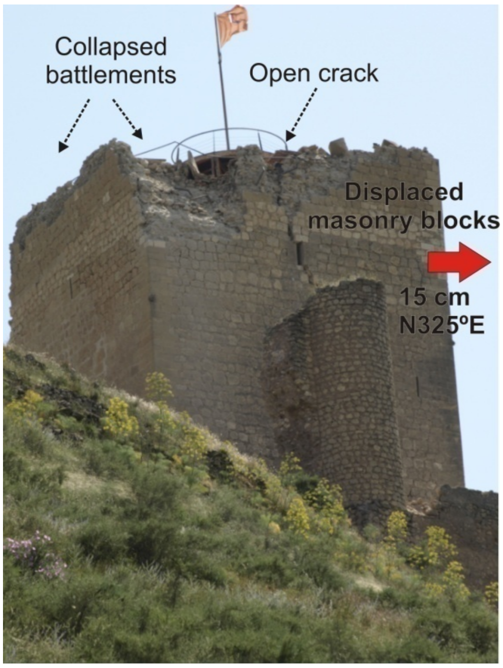

Fig. 5.3. EAEs affecting the "Espolón" tower in the Castle of Lorca. Generated by the earthquake of 2011/05/11.

Fig. 5.4. Displaced masonry block in the base of a column inside the "Espolón" tower in the Castle of Lorca (15 cm towards N325°E).

All of these collapses were restored after the earthquake and it is not possible observe them today. The penetrative cracks in walls appeared in the old Jewish quarter within the fortress and in the hermitage. The most important penetrative crack was developed in the "*El Espolón*" tower, located at the northeast part of the castle (Figs. 5.1; 5.4) (Giner Robles et al., 2012; Rodríguez-Pascua et al., 2012). This tower was damaged by another EAEs like displaced masonry blocks. The NW corner of the tower was displaced 15 cm (towards N325ºE) respect the base of the tower. This displacement is possible be observed today, after the restoration, in the first floor inside of the tower (Fig. 5.5). This displacement is compatible with the direction of movement calculated in the downtown of Lorca (Giner Robles et al., 2012; Rodríguez-Pascua et al., 2012). The battements were completely collapsed and destroyed; all of them were not original and, after the restoration, were eliminated. The "Alfonso X" tower only was EAEs in the top of the building with displaced masonry block, restored after the earthquake.

Acknowledgements: *Work funded by the Spanish Research Projects CGL2012-37581-C02-01 (QTECTBETICA - USAL). This work is a contribution of the Spanish Working Group of the INQUA TERPRO Project 1299 (EEE Metrics).*

Stop 6: Tebar Castle. Los Arejos Tectonic corridor: Pleistocene kinematics from bedrock fault-scarp exposures. Murcia.

M.A. Rodríguez-Pascua. *Instituto Geológico y Minero de España (IGME). marodriguez@igme.es*
P.G. Silva. *Dpt. Geology, University of Salamanca (USAL), Spain. pgsilva@usal.es*
T. Bardají. *Dept. Geology. University of Alcala de Henares (UAH), Spain. teresa.bardaji@uah.es*
E. Roquero. *Dpt. Edaphology, Technical University of Madrid (UPM), Spain. elvira.roquero@upm.es*

Los Arejos Tectonic Corridor constitutes the main boundary between the Eastern Betic Shear Zone and the Aguilas Arc. It can be considered as the prinxipal displacement zone (PDZ) along which took place the process of tectonic indentantion of the Aguilas Arc (Larouziere et al., 1988; Silva et al., 1993). As illustrated in figure 4.2 the prominet Almenara Range is separating these two main crustal-scale tectonic structures.

Prominent fault gouges develop along the western fault zone of Los Arejos Corridor, including highly deformend triassic Alpujarride metamorphics and Neogene sediments (manly Serravallian). The Tebar Castle fault zone is located in the central segment of the corridor after the progressive eastwards bending of the fault zone delineating the arched geometry of the fault zone consequence of the tectonic indentation processes. In this area the fault zone as a overall N70 -90E orientation and the existing outcrops display well developed subvertical bedrock fault scarps of c. 20 cm in height strongly dipping (>70º)to the east (Fig. 6.1). Preserved fault scarps are largelly exhumated to the NE due to quarrying during the 20th century.

Fig. 6.1. Bedrock fault scarp on Triassic limestones in contact with well cemented Pleistocene colluvial deposits.

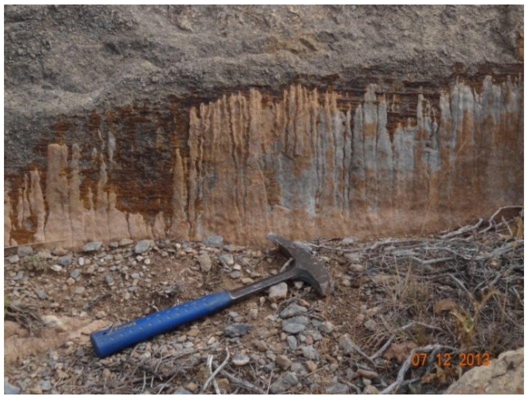

Fig. 6.2. Close-up view of the fault plane displaying the two nearly orthogonal sets of fault striae. The second striae set (subvertical) is overprinted on the frist one (subhorizontal), indicating an abrupt kinematic change in between.

The fault zone put in contact mylonitic neogene and metamorphic materials with triassic limestones and dolostones corresponding to the Alpujarrian units of the Aguilas Arc. The fault gouge is buried by well cemented colluvial deposits of apparent Pleistocene age (Silva and Bardají, 2013). These cemented deposits directly contact the triassic carbonatic materials upwards the fault plane where bedrock fault scarps occur (Fig. 6.1).

In detail, the fault plane displays two nearly orthogonal sets of fault-striae. The first striae set (older) is nearly subhorizontal and directly develop on the triassic materials (Fig. 6.2). The second striae set (younger) is nearly vertical,and is clearly overprinted on a thin (mm) calcrete coating the subvertical fault plane. Similar subertical fault planes and striae develop in the cemented colluvium in which the older subhorizontal fault striae set is absent. In most of the cases karstification processes operating on the fault planes after the formation of the younger subvertical striae resulted in the development of micro karren-like features enhacing this second fault striae set.

In consequence, geometrical relationships between the two fault striae sets record a significant kinematic change in the fault zones bounding the Aguilas Arc from Neogene to Pleistocene times. Subhorizontal striae developed in the triassic bedrock hae to be related with relevant, nearly pure, strike-slip tectonics driving the tectonic indentation of the Aguilas Arc, at least from post-Serravallian times (e.g. since the Tortonian). On the contrary the younger subvertical striae set is clearly related with the present morphotectonic framework and presumably linked to the development of the present morphology within Los Arejos tectonic corridor. The process can be linked to the post-indentation extensional collapse of the entire Aguilas Arc, which onset is dated in the Late Pliocene in the internal basins, such as the Cope Basin (Bardají et al., 2001). From the Middle to the Late Pleistocene, horizontal deformation shifted northwards, and presently the “indentation front” can be considered to be located in the Lower Segura thrust-blind fault (Fig. 6.3). In fact seismic records within the Aguilas Arc are really modest in comparision with the larger seismicity levels and younger deformation recorded in the Lower Segura Depression (Alfaro et al., 2012) at the northern terminal splay of the Eastern Betic Shear Zone (Fig. 6.3), where the relief of the Carrascoy range and the Lower Segura fault are clearly post-messinian (Silva et al., 1993).

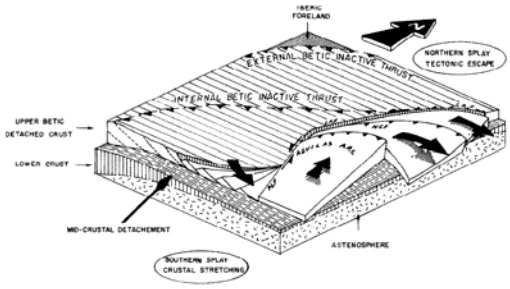

Fig. 6.3. Schematic block diagram showing how lateral slip along the central segment of the Eastern Betic Shear zone is compensated by thin-skinned thrusting and shallow, crustal level, tectonic escape in the Lower Segura Depression (North) and shallow crsutal stretching and Horse-tail splay fault assemblages in the South (i.e. Almanzora Tectonic Corridor and Almería Basins). From Silva et al., 1993.

However, still in the Aguilas Arc compressive tectonics occur and Late Pliocene sedimentary sequences to Late Pleistocene marine terraces (stop 7) are gently folded. In this sense it is to note that geodetic studies in this zone indicate that in spite of this low seismic activity, the internal ENE-WSW to E-W thrusts of the Águilas Arc yield the highest uplift-rates in the Eastern Betic Cordillera, with maximum values of 0.95 ±0.2 mm (Giménez et al., 2000). These authors used leveling-lines from 1934 to 1976 to detect a positive asymmetric anomaly of 40±8 mm south of Águilas coinciding with the southern termination of Los Arejos Tectonic Corridor.

Fig. 6.4. View of the ground surface rupture at the Teber Castle zone

On the other hand, the preservedfault scarp in the Tebar Castle zone has a really nice geomorphological expression, being possible to follow the surface rupture over a length of about 1 km (Fig. 6.4). The question here is to consider if the apparent fresh ground rupture is merely preserved because the indurate nature of the bedrock and colluvial deposits or if we are looking to a historical earthquake surface rupture.

Acknowledgements: *This work has been funded by the Spanish research Projects CGL2012-37581-C02-01(QTECTBETICA - USAL), and CGL2012-33430 (CSIC), It is a contribution of the Spanish Working Group of the INQUA TERPRO Project 1299 (EEE Metrics).*

Stop 7. Cope Basin: Soft-sediment deformations and anomalies in height distribution of Last Interglacial to Holocene marine terraces. Murcia

***T. Bardají**. Dept. of Geology, Geography and Environment (UAH, Spain). teresa.bardaji@uah.es*
***A. Cabero**. Fac. of Sciences (UNED, Spain). acabero@ccia.uned.es*
***P.G. Silva**. Dpt. Geology, University of Salamanca (USAL), Spain. pgsilva@usal.es*

Cope basin is a small littoral plio-pleistocene sedimentary basin located in the inner part of the Aguilas Arc, where the N-S shortening produced by blind-faults at depth is partially accommodated by the generation of more recent NE-SW (N120E) strike-slip oblique faults (Bardají et al., 2014), as presently occur in the Lower Segura Fault (Alfaro et al., 2012). This set of faults governed not only the sedimentation and relief patterns during the Middle-Late Pleistocene within the Cope Basin but also the spatial and altitudinal distribution of Pleistocene marine and terrestrial units (Bardají et al., 2010),. The two most prominent tectonic structures of the basin define its northern compressive margin as in contact with the Betic metamorphic substratum, La Galera (NE-SW) and La Panadera (E-W) faults, (Fig.7.1).
N120E and N60E faults led to the opening of the Cope Basin, where data from boreholes indicate that no sedimentary materials were deposited during pre-Pliocene times (Bardají et al., 2010; Silva et al., 1993; 2003). The first Pliocene series comprises submarine basalts and fine-

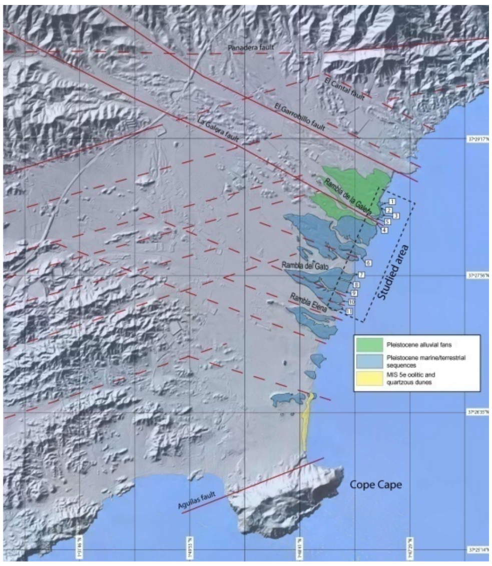

Fig. 7. 1. Cope Basin. Main faults and distribution of Pleiatocene units

grained marine blue clayey-silts (> 100 m thick), which evolve upwards to littoral sequences of sandy-silts and gravels to the eventual deposition of Plio-Quaternary marls and dominantly yellow fossiliferous calcarenites (c. 50 m thick).

These yellow calcarenites are deformed by NE-SW to ENE-WSW large folds of hectometric wavelength and metric amplitude with low dip (<15º). These materials are unconformably overlain by a well-cemented NW-NE offlapping Pleistocene sedimentary sequence where shallow marine and coastal sediments alternate with sub-aerial alluvial fans (Bardají, 1999; Dabrio et al., 1991; Zazo et al., 2013). The arrangement of this sedimentary sequence is mainly conditioned by the more recent N120E fault system, but differential inland uplift along the Quaternary resulted in a seawards-offlapping (NE-SW) arrangement of the sedimentary sequence.

Sedimentary sequence and reconstruction of sea level history.

The most recent units of the general sequence are slightly staircased into the former ones, and they have been attributed to MIS7-MIS5 mainly by their faunal content and sedimentary facies, (Bardají et al., 2009; Zazo et al., 2003, 2013).
In order to reconstruct the sea-level history we have considered the following sea-level geomarkers (accuracy): inner edge of marine unit (±1-1.5m), plunge step (0m) and shore-line angle/notch (±0.5m).

Up to six sedimentary units have been described for this MIS7-MIS5 sequence (Fig. 7.2), however, only three of them (Units B, C and D) appear widely exposed along the basin. The complex distribution of these units is interpreted as the consequence of the joint action between sea-level changes and seismotectonic activity (Bardají et al., 2013; 2014).

Unit A: Plio-Pleistocene marine yellow calcarenites with an erosional wave cut platform on top (a in Fig.2).
Unit B: MIS7 yellow fine-bedded foreshore-shoreface (plunge step) calcarenites alternating with gravel levels (both coastal and continental origin) of variable thickness. At least two different prograding sub-units have been identified.
Unit C: Erosive terrestrial unit, with two different facies patterns: purple-grey gravels and fine grained laminated purple dolomitic muds; several beach sand levels develop on top of the unit. The age of this unit has been assumed to be the end of MIS 6 under rising sea level conditions.
Unit D: MIS 5e coastal grey conglomerate with rounded quartz pebbles, cobbles and boulders. Faunal content corresponds to *Glycymeris* and *Ostrea*, with a few individuals of *Strombus bubonius, Thais haemastoma* and *Conus* sp.

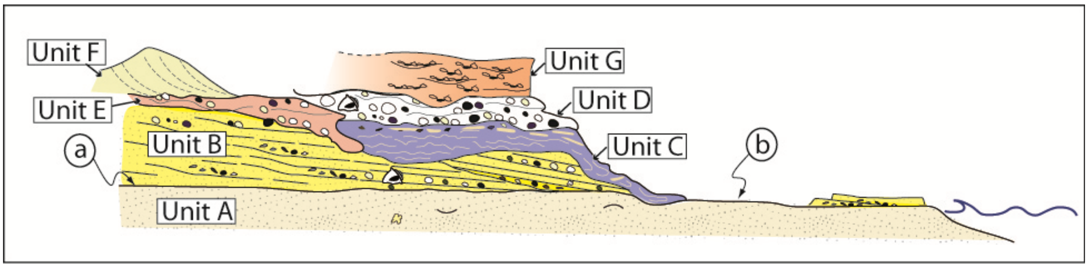

Fig. 7.2. Synthetic sedimentary sequence (after Bardají et al., 2014). Explanation of units in text

Three different sub-units (highstands) have been identified.

Unit E: Conglomerate with rounded quartz pebbles with reddish clayey matrix (backshore facies). Locally, it covers terrestrial deposits of Unit C. In the southern zone it underlies last interglacial quartzous dune (F).

Unit F: Quartzous aeolian dune with some reworked oolites. These dunes and the oolitic ones only outcrop in the southern part of the basin.

Unit G: Reddish gravels from lowstand alluvial fan systems overlying the sequence in the northern sector. Spatial distribution of these deposits as well as the age of underlying marine unit (MIS 5e) point to a probable Last Glacial age for this unit although MIS 5b/d age can not be discharged.

A younger cliff and wave cut bench (b in Fig. 2) cutting the whole sequence represent a younger and steady sea level. The age of this last highstand can be attributed either to MIS 5a or to the Holocene.

maximum values of 0.95 ±0.2 mm (Giménez et al., 2000). These authors used levelling-lines from 1934 to 1976 to detect a positive asymmetric anomaly of 40±8 mm south of Águilas.

In spite of this low instrumental or historic seismic record, probable paleoseismic evidence was found at Renco coastal sector, all within the terrestrial sedimentary Unit C (see Fig. 2). The palaeoseismic structures consist on:

- Pervasive soft-sediment deformation structures in the fine facies (mud) of terrestrial Unit C.
- Flow or slump-like structures that spread over the ancient cliff and above the former wave-cut bench "b.

These structures point to a seismic intensity of at least VIII after the ESI-2007 Scale, much higher than the maximum values recorded in the Aguilas Arc (IV-V MSK).

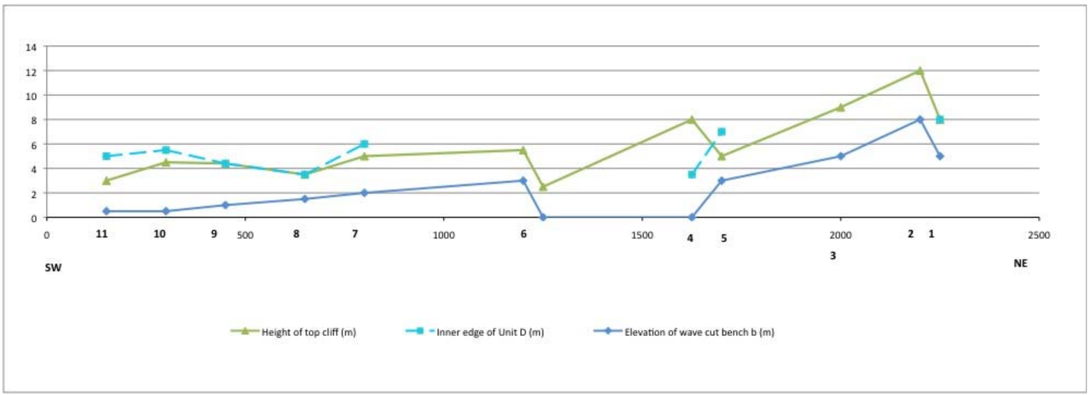

Fig. 7.3. Heigth distribution of key geomorphological features (after Bardají et al., 2014)

Paleoseismic structures.

Although only few low magnitude instrumental earthquakes (≤ 4.0 Mw) and two historic earthquakes (Águilas, AD 1596 and AD 1882), with maximum intensities of IV-V MSK (Mezcua, 1982; IGN, 2014), geodetic studies in this zone indicate that the internal E-W to ENE-WSW thrusts of the Águilas Arc yield the highest uplift-rates in the Eastern Betic Cordillera, with

Height distribution of wave-cut bench b.

The heights of the sea level geomarkers described above, specially the height of the inner edge of Unit D and the height of the wave-cut bench "b", were measured and plotted in order to analyse the differential uplift of faulted blocks (Bardají et al., 2014). These record apparent large wave-length folding in the southern sector of the basin, but short wavelength folding and subsequent faulting in its northern sector (Fig. 3). Since the wave-cut bench analysed is an erosive rocky landform lacking any possible ductile behaviour, apparent folding results in subsequent ground ruptures which are mainly accommodated along the N120E fault system which governs the present landscape assemblage.

Having into account the assumed age of the wave cut bench (MIS 5a – Holocene) the calculated slip rates range between 0.016 mm/yr (since MIS 5a) to 0.15 mm/yr (since middle Holocene).

Acknowledgements: *Work funded by the Spanish Research Projects CGL2012-37581-C02-01 (QTECTBETICA - USAL), CGL2012-33430 (CSIC), CGL2013-42847-R (UNED) and ACI-2009-1037. This work is a contribution of the Spanish Working Group of the INQUA TERPRO Project 1299 (EEE Metrics), IGCP Project 588 and INQUA CMP WG on Long Term Sea-level Changes.*

Fig. 7.4. Field image and thin sections of the fluidized deposits (Unit C) displaying coseismic soft-sediment deformation structures (after Bardají et al., 2014)

Stop 8: The Alhama de Murcia Fault (AMF): The fault gouge at the La Torrecilla Rambla, seismogenic implications.

***J. J. Martínez-Díaz**. Complutense University of Madrid, IGEO (UCM-CSIC) jmdiaz@ucm.es*
***E. Rodríguez-Escudero**. Dpt. Geology and Geochemistry, Autonomous University of Madrid (UAM) emilio.rodriguez@uam.es*

The Alhama de Murcia Fault

The Alhama de Murcia Fault (AMF) is a NE-SW sinistralstrike-slip fault with reverse component and NW-dip that cross the Internal Zones (or Alborán Domain) of the Eastern Betics Cordillera (Fig. 1.1). Along its ~100 Km long trace the AMF bounds the Guadalentín Depression and the mountain ranges that elevate on the northwestern margin (Las Estancias, La Tercia and Espuña Ranges; Silva et al. 2003). This mountain fronts are controlled by the tectonic activity of this fault that extends from the late Miocene to present, determining both the evolution of the Guadalentin depression and some Neogene basins (Huércal-Overa Basin, Lorca Basin and Fortune Basin; i.e. Meijninger, 2006).

The AMF is part of the Eastern Betics Shear Zone (Silva et al., 1993) than includes several large fault zones: Palomares, Carboneras, AMF, Carrascoy and Bajo Segura faults. The AMF accommodates part of the convergence between Africa and Eurasia (Masana et al., 2004), recent gps studies indicate that most of the deformation is concentrated in this sector on the Alhama de Murcia fault. They estimate a reverse-sinistral geodetic slip rate of 1.5±0.3 mm/yr for this fault (Echeverria et al. 2013). Instrumental seismicity is characterized by shallow earthquakes of low to moderate magnitude capable to generate enormous damage such as the 2011 Mw 5.2 Lorcaearthquake (Martínez-Díaz et al., 2012).

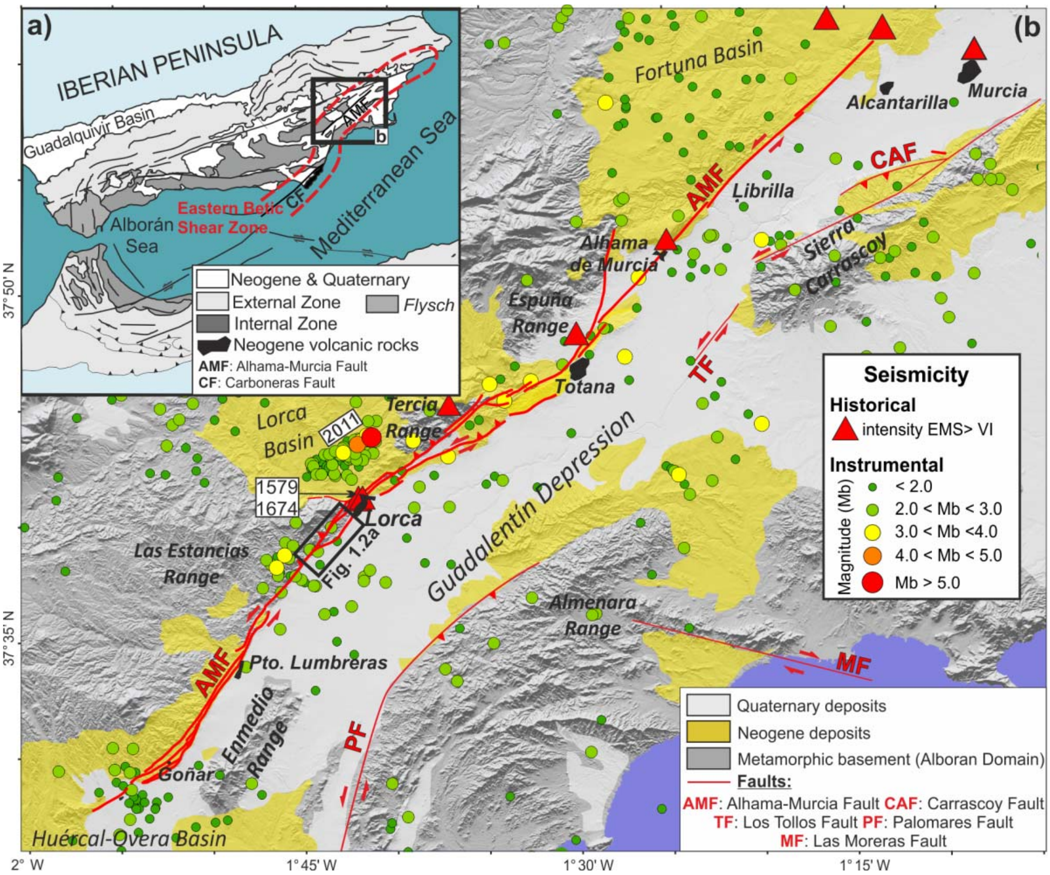

Figure 8.1: a) Structural-tectonic sketch map of Betic-Rif Cordillera, the Eastern Betics Shear Zone is marked by dashed red line. b) Geological map of the Eastern Betic Cordillera with the historical and instrumental seismicity associated with the Alhama de Murcia Fault. White squares indicate dates of historical earthquakes occurred next to Lorca, and the 2011 Lorca seismic series. Seismic data from the Instituto Geográfico Nacional and from the Instituto Andaluz de Geofisica

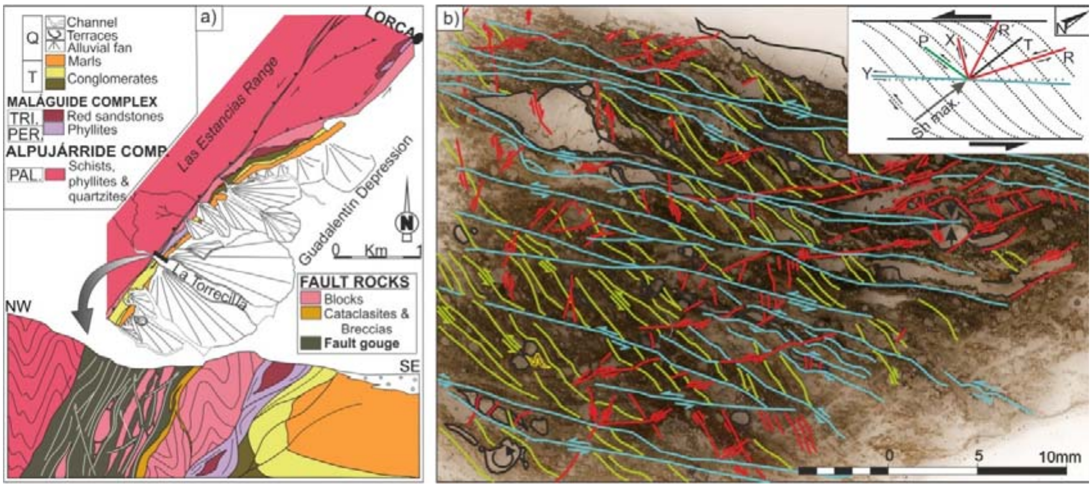

Figure 8.2: a) Outline geological map of the AMF in SW Lorca (situation in Fig. 1.1-b) and a schematic cross section of the damage zone of the AMF along the Rambla de La Torrecilla. b) Microstructural interpretation of a horizontal thin section of the fault gouge. In the right corner is shown the angular relationship between Riedel fractures observed in the gouge and AMF-trend showing a sinistral sense of motion and a NNW-SSE orientation for the maximum horizontal shortening (Shmax.).

In addition, several historical earthquakes of EMS intensity greater than VI (i.e. 1579 and 1674) are attributed to the AMF in the last 500 years, and paleoseismic studies expose the occurrence of several prehistoric events of Mw magnitude greater than 7 (Martínez-Díaz et al. 2001; Masana et al, 2004; Ortuño et al, 2012).

The shear deformation along AMF brought into mechanical contact the Betic metamorphic basement that outcrops in the mountain ranges with Miocene and post-Miocene deposits that fill the Neogene basins (Fig. 8.1). The shear zone along these contacts produces a very heterogeneous fault zone consisting of several shear planes that adopt a braided morphology typical of strike-slip faults (Silva et al. 1992).
The fault zone shows a spectacular tectonic banding where breccias, cataclasites and fault gouges are frequent. It has been observed in several outcrops of the AMF between Puerto Lumbreras and Totana that the development of fault gouge is restricted to contact between schists and phyllites of the Betic basement. The fault gouge has been linked mineralogically with these lithologies using XRD analyses (Rodríguez-Escudero et al., 2014). The structure of the AMF at seismogenic depth (several km), should be restricted to schists and phyllitesfrom Betic basement. the study of fault gouges generated in these materials is then very important to understand the seismogenic behavior of the AMF

Fault gouge at the La Torrecilla Rambla.

The incision caused by the Rambla de La Torrecilla on the southeastern front of Las Estancias Range offers a spectacular outcrop of the damage zone associated to the AMF (Figs. 8.2 and 8.3). In this area the AMF warps different rocks of the Betic basement and Neogene deposits and the drainage network, however, the most distinctive feature is the development of a clayey fault gouge band of ~10 m wide in sharp contact with graphitic schists of the Betic basement. This gouge band is divided to NE in Riedel-geometry branches of decimetic scale that individualize large protolith blocks. The gouge is composed of a grayish cataclastic matrix containing angular and sigmoid-shaped protolithclasts. XRD diffraction analyses of samples show that the gouge and clasts are mainly composed of phyllosilicates and quartz with lesser amounts of carbonates, graphite and Fe-oxides.

The fault gouge from La Torrecilla is known and studied since the 80´s for its spectacular ductile-style textures that show a sinistral-reverse kinematics (Rutter et al, 1986, Oliveros, 1987, Martinez-Diaz, 1998; Rodríguez-Escudero et al, 2012). Often, these textures are molded by pulverized quartz clasts with "icing sugar texture", compound by sub-millimetric particles that becomes powder when agitated. Although ductile-shaped textures can be interpreted to have been derived from ductile fault rock formed at large depths, the microtectonic analysis of the gouge shows a fragile origin for these textures, caused by sets of conjugate Riedel-fractures under a brittle regime at shallow depths (<10Km; Rodríguez-Escudero et al., 2012). The orientation of these fractures is similar to meso- and macro-scale field observations, allowing to determine a NNW-SSE orientation for the maximum horizontal shortening axis (Shmax.; Fig. 8.2), which is reliable with the current regional strain field (Martínez-Díaz, 2002

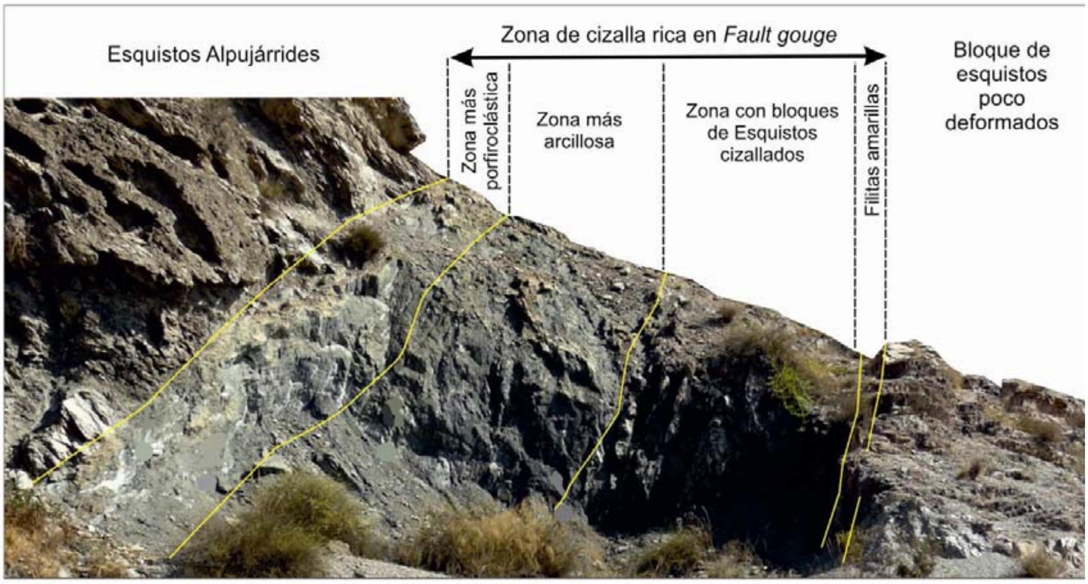

Figure 8.3. Field view of a cross section of the fault gouge at the La Torrecilla Rambla as it can be observed in stop 8

Seismogenic implications.

Microtectonic analysis of the fault gouge reveals a mixed slip behavior for the AMF dominated by long periods of seismic calm (controlled by aseismic deformation mechanisms) that are eventually interrupted by seismogenic mechanisms. Development of ductile-style textures at shallow crustal levels generally involves very slow deformation processes that could be coherent with slip by aseismic creep for this section of thee AMF (Rodriguez-Escudero et al., 2012). However, the presence of pulverized quartz clasts has been interpreted as a coseismic effect produced by a normal stress drop when seismic waves passing through the fault rocks (Rodríguez-Escudero et al., 2014).

Presence of fault gouge along the AMF is not only a good record of past seismotectonic activity; it can also determine the seismogenicbehavior of this fault in the future. Niemeijer&Vissers (2014) recently studied the frictional properties of the fault gouge from the epicentral zone of the 2011 Lorca earthquake and observed that it could have been partially responsible for the rupture directivity to SW during the mainshock. Also, the geometry of the fault gouge fabric is dominated by Riedel-planes affecting schists in the epicentral area. These planes are parallel to the nodal plane obtained by López-Comino et al. (2012) for the focal solution of the main events of the 2011 Lorca series. The gouge of the AMF is usually divided in Riedel-oriented branches and it is structured in bands of decimeter to decametric width that bound large protolith blocks. Where the gouge thickness is reduced to zero two protolithblocks are in contactresulting in an asperity capable to accumulate stress and to generate seismic slip.

On the contrary, it has been observed that the presence of graphite in fault gouges could play a mitigating role (Oohashi et al., 2013). Graphite reduces the frictional properties, facilitating the aseismic sliding and inhibiting the nucleation of large earthquakes.

A PhD Thesis is in progress with the aim to investigate in more detail the mechanical properties of the fault gouge and the internal structure of the AMF in order to increase the knowledge about the seismogenic behavior of this fault.

Acknowledgements: *This work has been founded by the Spanish research Project CGL2013-47412-C2-1-P (INTERGEO).*

Stop 9: El Saltador Rambla: An overview to the seismic landscape of the Lorca-Totana fault segment (AMF) and Tectonic Geomorphology of Alluvial fans.

P.G. Silva. Dpt. Geology, University of Salamanca.pgsila@usal.es
T. Bardají. Dpt. Geology. University of Alcala de Henares (UAH), Spain. teresa.bardaji@uah.es

The Guadalentín Depression (Murcia, SE Spain) constitutes one of the Quaternary sedimentary basins developed along the set of NE-SW active strike-slip fault systems of the Eastern Betic Shear Zone (EBSZ: Larouzière et al. 1988, Silva et al. 1993). This tectonic depression, more than 100 km in length, is one of the most outstanding examples of recent tectonic landscapes in the Betic Cordillera, subject to well documented historical and present seismic activity (Mw 5.1 2011 Lorca Earthquake; Alfaro et al. 2011). The depression is bounded by faulted mountain fronts which provide evidence of an important Late Quaternary tectonic activity (Fig. 2.1) linked to the development of a large variety of tectonic landforms of mostly strike-slip origin (i.e. micro pull-apart basins, lineal sag ponds, spur ridges, drainage offsets, etc. (Silva, 1996; 2013; Silva et al. 1992a, 1997, 2003, Martínez-Díaz et al. 2012). Tectonic activity of mountain fronts is well recorded in nice proximally trenched to distally aggrading alluvial fan sequences, whose geomorphological assemblage provide evidence on (a) their uplift history (Harvey 1984, Silva et al. 1992b); (b) the progressive installation of the drainage network during the Late Quaternary (Harvey 1990, 1997); (c) and the transition from alluvial to fluvial systems in the semiarid SE Spain during historical times (Silva et al. 1996, 2008, Calmel-Avila, 2002).

The interaction among tectonics, climate and alluvial sedimentation allow the development of widespread set of tectonic landforms and alluvial fan surfaces with different degree of calcrete development and morpho-sedimentary assemblages witnessing the different styles of faulting and uplift history of the associated range front faults. Large fans generate in the major fault-gap segments at basin margin locations (i.e. Lorca Fan). The preserved Late Holocene alluvial landforms and sedimentary sequences within the depression offer a first quality geoarchaeological record illustrating the relationships between the human populations and drainage changes and reorganization since the early Bronze Age to Medieval times (Silva et al. 2008).

Alluvial fan sequences in the Guadalentin Depression.

Alluvial fans are the most extensive landforms occurring in the Guadalentín Depression. Small to medium fan systems develop in the main faulted mountain fronts, whilst extensive larger fans (i.e. Lorca, Nogalte, Lebor, Algeciras and Librilla) develop from the drainage gaps existing between the different fault segments (Fig. 9.1) defining the main range fronts. Alluvial fan development in this region display a complex Pleistocene history (Harvey 1990, Silva et al. 1992b) with (a) early periods dominated by aggradation, followed by (b) fan-surface

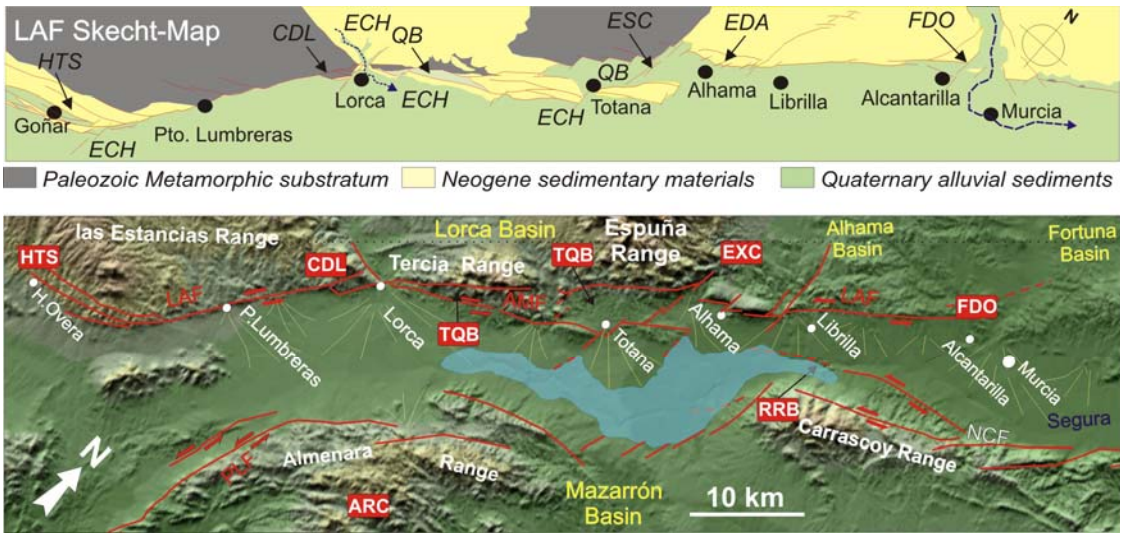

Fig. 9.1.Geomorphological and tectonic setting of the Guadalentín Depression. Red: main strike-slip fault systems of the region working as major range-front faults. Yellow: location of the main Late Neogene sedimentary basins. White: main ranges and localities of the region. Shaded blue zone: ancient palustrine area. PLF: Palomares Fault; NCF: North-Carrascoy Fault; LMF: Las Moreras Fault; ARC: Aguilas Arc; LAF: Lorca-Alhama de Murcia Fault;HTS: Horse tail splay termination of the LAF; CDL: ContractionalDuplex of Lorca; TQB: Triangular Quaternary basins (pull-apart); EXC: Extensional system of Canacarix; RRB: El Romeral rock-bar fault; FDO: Fault die-out at surface.

stabilization and calcrete-crust formation (Alonso Zarza et al. 1998) and eventually (c) fanhead trenching and distal aggradation (Silva et al. 1992b). These works identified different sedimentary styles in alluvial fan deposition related to different mountain front geomorphology, lithology and degree of tectonic activity in the related range front fault segments, allowing to discriminate three main depositional alluvial fan sequences along the entire Guadalentin Depression (Fig. 9.2).

a) The first depositional phase dominated by cemented debris-flow conglomerates, with development of thick calcrete profiles at surface (Alonso Zarza et al. 1998) can be assigned to the middle Pleistocene with a minimum age of > 330 ka on the basis of available age data along the fault zone (Shobati et al. 2011, Ortuño et al. 2012). This phase is clearly syntectonic displaying a relevant proximal offlap progressive unconformity related to relevant continuous uplift along the oblique-slip range front faults. Geomorphological expression of this oldest fan surfaces is dominant in the southern horse-tail splay termination of the fault (Goñar) and the proximal zones of the intervening strike-slip triangular basins developed in the branched central sector of the AMF between Lorca and Alhama de Murcia.

b) The second depositional phase comprised by debris-flow and “fluvial” conglomerates and sands with a sedimentary style of proximal

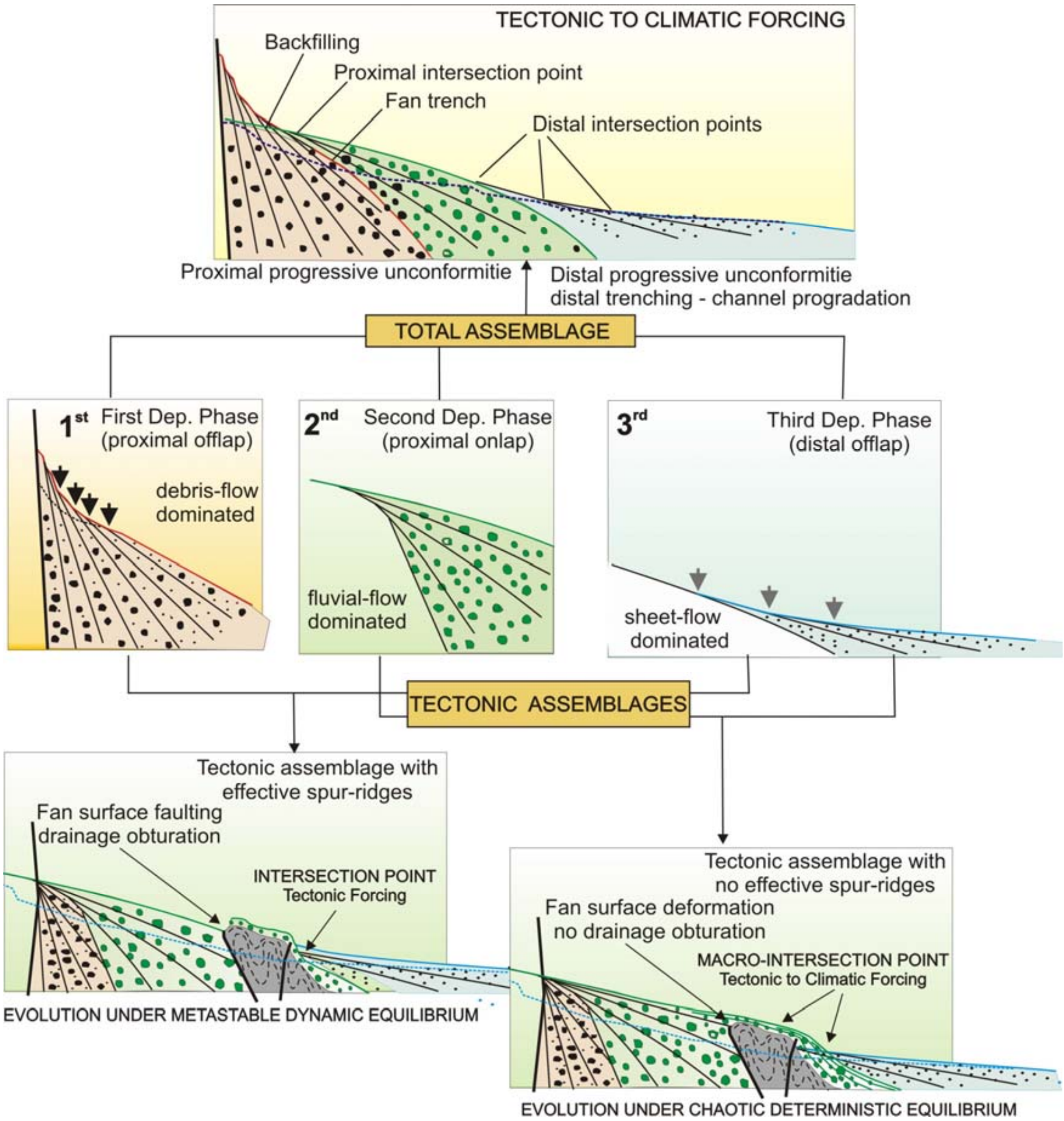

Fig. 9.2.Assemblage and characteristics of alluvial fan bodies along the margins of the Guadalentín Depression illustrating tectonic and climatic forcing from the Middle Pleistocene to the Holocene during the deposition of the three main depositional sequences identified in the zone. Complex Tectonic assemblages illustrate cases recorded in the Lorca-Totana fault segment (modified from Silva, 2013).

onlap, eventually gave place to proximal fan aggradation and backfilling on the mountain front catchments. Fan surfaces of this phase display some degree of cementation, but no true calcrete development (Alonso Zarza et al., 1998). Recent Age data (Shobati et al., 2011, Ortuño et al., 2012) allow to assign this phase to the Middle-Late Pleistocene, with bracketed ages of 290 to 106-107 ka. In this case, final elaboration of fan surfaces by means of proximal onlap aggradation and backfilling can be preliminary assigned to the last interglacial period (MIS 5). Fan surfaces of this second depositional phase are those dominating the entire mountain fronts from the southern and central sector of the depression. Proximal onlap aggradation can be interpreted as a progressive buffering of tectonic uplift along the range-front fault zone.

c) The third depositional phase mainly comprise sandy to gravelly sheet flood deposits, with inset channelled fluvial gravels generated by the successive set of dichotomic distributary systems. This phase is characterized by the development of proximal fanhead trenches and a sedimentary style of progressive distal aggradation, with the generation of successive distal intersection points and the development of prograding telescopic fan systems into the endhoreic environments located in the center of the depression. Available age data (OSL, Th/U, C^{14}) from geo-archaeological (Calmel-Ávila, 2002, Silva et al., 2008) and paleoseismic research (Martínez Díaz et al. 2003 Massana et al. 2004; Ortuño et al. 2012) allowed a finer subdivision of the third depositional fan sequence in several Late Pleistocene (< 100 ka BP), Early Holocene, Bronze, Roman, Muslim, and historically recent phases of distal fan aggradation (Silva et al. 2008).

Chronology of alluvial fan sedimentation

In detail analyses in the larger fans generated from during the Holocene (Fig.9.2) indicate that truly palustrine environments prevailed until ~4,500 – 4,300 yr BP. However, dominant endorheic conditions remained until the Late Calcolithic period (~2800 BC) when the first evidence of dissection is observed in the northern sector of the depression in the Librilla and Algeciras ramblas (Calmel-Avila 2000, 2002). Major intrabasinal incision events did not take place after~2,400 – 2,000 BC (Early Bronze Age), when relevant headward erosion reached the central sector of the Guadalentín Depression between Librilla and Totana (Fig. 9.3), inducing an incision up to 17m (Calmel-Avila 2002). Semi-endorheic conditions remained in the centralmost zone of the depresion (Totana zone, Fig. 9.1) until the 16th to 17th centuries. In this zone the ancient palustrine environments were fragmented by fluvial dissection from the Early–Late Bronze transition evolving to smaller and ephemeral playa-lake systems, and causing a relevant depopulation of the zone (Calmel-Avila, 2002; Silva et al., 2008).

Environmental and population changes during the Bronze Age seems to coincide with the activity of the northen prolongation of the southern branch of the AMF beneath the sedimentary filling of the depression at El Romeral Rock-Bar Fault near Librilla (Fig. 2.1). In this site the nearly entire Early Holocene palustrine sedimentary sequence is tilted about 16º SW (Calmel-Avila, 2002) against the fault. Recent archaeoseismological research in the Late Bronze site of La Tira del Lienzo (near Totana) record an apparent surface faulting event (5.7 – 6.0 Mw) ~1,550 BC (Ferrater et al., 2014; en prensa). Consequently these preliminary data may suggest that the onset of true fluvial dissection within the depression was a relevant secondary effect o fault activity of the southern branch of the AMF.

Tectonic Geomorphology of the Central Segment of the AMF.

This stop is located in the central segment (Lorca-Totana) of the AMF fault zone. The main feature of this segment is the occurrence of fault branching between Lorca and Alhama de Murcia, giving place to a set of intervening contractional duplexes (i.e. Lorca CDL), triangular strike-slip basins (TQB), and small pull-apart zones in which the Pleistocene fan surfaces are uplifted and faulted generating kilometric spur-ridges, linear tectonic ridges, beheaded fans and channels as well as small scale horst-graben topographies linked to N-S extensional structures.

The main tectonic feature is the generation of the triangular strike-slip basins (La Hoya and Totana basins; Fig. 2.1), where commonly the oldest alluvial fan sequences are confined. Fan sequences filling these basins belong to the first and the second depositional phases described above. First phase fans are totally confined within the basins, but early sedimentation of the second depositional phase coincides with the generation of intervening tectonic reliefs (spur ridges) in which fan deposits are incorporated and fan surfaces faulted and/or deformed in the top of these linear reliefs (Fig. 9.2). Therefore, surface activity of the AMF southern branch started about 300 - 290 kyr BP, during the end of the Middle Pleistocene. Consequently the related tectonic landscape observable nowadays (Fig. 9.3) is really young, since the more relevant episodes of fanhead trenching leading to distal fan progradation into the depression can be assigned to the Last interglacial period about 100 kyr BP (Silva, 2014).

Differences in elevation between the earlier fan surfaces of the second and the third depositional phases related to the intersection points of the fans (internal base levels) are about 70 – 80 m (Fig. 9.2.). These values can be considered as

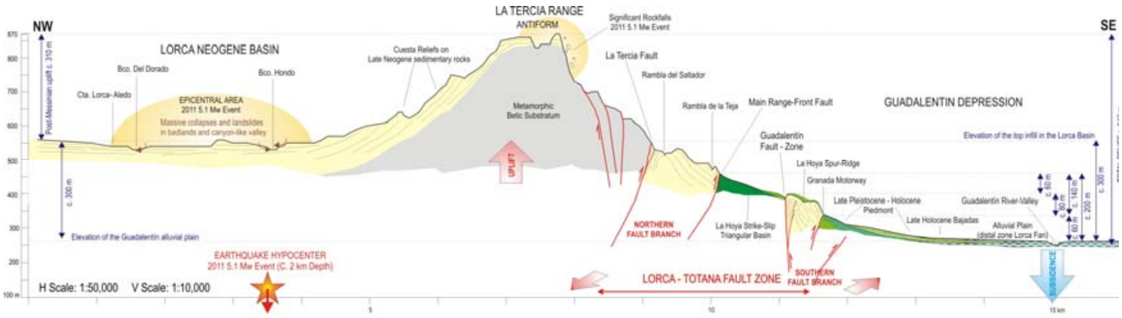

Fig. 9.3.Geomorphological cross-section of the Lorca-Totana fault segment illustrating fault branching in the AMF and elevation differences between the most significant geomorphological surfaces in the zone. Also most significant zones affected by secondary coseismic effects (slope movements) during the 2011 5.1 mw event are highlighted.

the minimum uplift recorded in this fault segment between 300 and 100 kyr BP, resulting in maximum uplift rates of about 0.4 to 0.35 mm/yr for that period. These inferences can be made because alluvial fans have internal base levels that in tectonically active areas are mainly controlled by tectonics. As abovementioned some of the fan surfaces of the second depositional phase surpassed the intervening tectonic reliefs, leading to the generation of macro-intersection points and triggering their accelerated dissection (Fig. 9.2). The accelerated incision is consequence of the tectonically induced step in the fan surfaces leading the fan channels work under a deterministic chaotic dynamics evolving towards full-dissection in the entire fan surface (Silva, 1994).

On the contrary, in those cases in which the intervening tectonic reliefs were effective shuttering the drainage by surface faulting (proper shutter ridges; Fig. 9.2), intersection point development and subsequent trenching is focused only in the main fan-channel. In this context headward erosion on the beheaded channel downstream the tectonic relief will control the incision process under a common dynamic metastable equilibrium. However, in inter-fan channel areas, drainage shuttering is effective and younger fan sediments can be recorded. This is the cause for which trenches developed in the southern branch of the AMF can record fan sediments younger than 100 kyr BP (Martínez-Díaz et al., 2003; Masana et al., 2004).

Figure 9.3 shows a transverse geomorphological section of the Lorca-Totana Fault segment, illustrating the assemblage of fan surfaces within the fault zone and elevation differences between the more outstanding geomorphological surfaces in the zone. These elevation differences help to get an idea about the total uplift of the zone triggered by the activity of the fault and relative uplift/subsidence processes occurred in the zone during post-Messinian times. Also the figure illustrate the location of the zone in relation to the epicentral area of the 2011 5.1 Mw earthquake and coseismic slope processes.

Acknowledgements: *This work has been funded by the Spanish research Project CGL2012-37581-C02-01 (QTECTBETICA-USAL).*

Stop 10: El Saltador fault-trenches: analysis for slip-rates and for paleoearthquakes

E. Masana, M. Ortuño, M. Ferrater, Barcelona University, eulalia.masana@ub.edu
J.J. Martínez Díaz, Complutense University of Madrid, IGEO (UCM-CSIC) jmdiaz@ucm.es

Nine new trench exposures were excavated at El Saltador site (6 km NE of Lorca, Fig. 1), six of them parallel to the fault (Figs. 2 and 3). Two previous trenches at this same site suggest the occurrence of two paleoearthquakes (Martínez-Díaz et al., 2003; Masana et al., 2004). The main objectives of these new trenches are a) to constrain the left-lateral slip-rate for the AMF by exposing linear features (i.e. paleochannels) that are offset by the fault, and b) to detect past paleoearthquakes and complete the sequence.

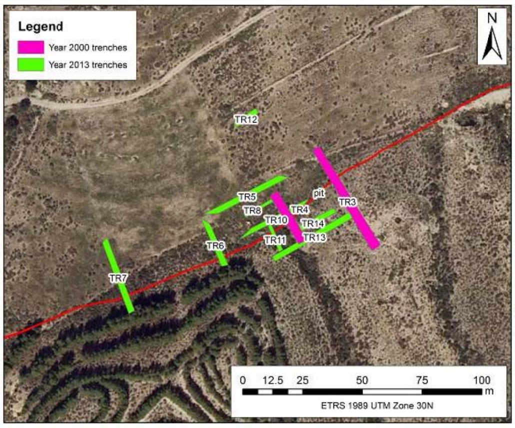

Figure 10.1.Aerial photo with the location of the trenches.

Fault slip-rate analysis

For the slip-rate calculation we measured the offset by detecting different piercing points in a buried channel system (Ferrater et al., 2014a). In the stratigraphic record such linear features are channels or their components, such as the channel margins. We interpret unit D to be a fluvial channel owing to its erosive base and its filling (Fig. 4). Unit D shows two laterally distinct lobes (Figs. 4 and 5). We used the lowest channel for the offset measurements because the morphology of this channel is clearer.

	3D distance	Map distance	Vertical distance
Rightbank	15.07	15.05	0.77
Depocentre	17.31	17.25	1.49
Leftbank (curvaturechange)	15.76	15.76	0.18
Leftbank (facies change)	18.18	18.17	0.68

Table1. Offset measurements (meters) for the channel.

We have measured the offset between the lines that constitute: 1) the two banks or margins; and 2) the channel thalweg. In the case of the banks, the measurement can be done using curvature criteria or facies criteria. We have estimated the trend of the channel by connecting the different outcrops of each feature considered. At least every feature has been identified in two or three trench walls. The measurement of the lateral and vertical offsets was made with the help of GoCAD 3D software and the previous measurements have been done using Excel worksheets. The following information was considered for the offset measurement: 1) the logs of the walls of trenches where unit D is exposed; 2) the interpreted unit D; 3) the Alhama de Murcia fault plane; and 4) a Digital Elevation Model (DEM) of the site.

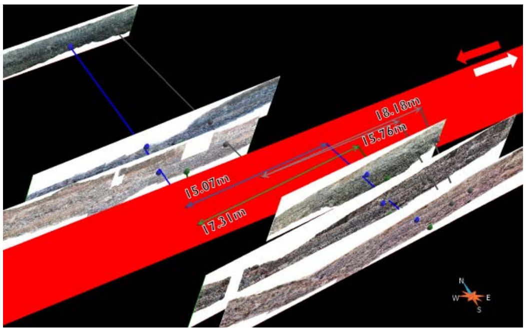

Figure 10.2. 3D model of the trenches 5, 10, 13 and 14 created with GoCAD software. This ongoing work interpretation allows the measurement of channels offsets. Measurements (3D) for the lowest D channel (Right bank = 15.07 m, Left bank for curvature criteria = 15.76 m, Left bank for facies criteria = 18.18 m, Depocentre = 17.31 m).

The total net offsets (table 1) for the considered channel range between 15.1 and 18.2 m. The lateral components are 15.0-18.2m (16.6-/+1.6m).

a) Dating. Dating of the units described in El Saltador site is still in progress. We gathered samples to be dated using ^{14}C, OSL (Optically Stimulated Luminescence), AAR (Amino-acid racemization) and U-series applied to pedogenic carbonate (see Ferrater et al., 2014b).

A Radiocarbon-dated charcoal sample taken from unit H (in trench 6, shown in Masana et al, 2014), yields a calibrated age of 23,883-23,279 B.C. (2σ interval). Unit H is stratigraphically lower than unit D (several units lower, Fig. 4), thus making unit D younger than 23,883-23,279 B.C.

b) Lateral slip-rate calculation. We obtain a minimum slip-rate, as we use a maximum age for unit D. The lateral slip-rate (15.1-18.2 meters in 21,210 years) is estimated to range between 0.63 and 0.78 mm/yr (Fig. 10.2).

Even being considered a minimum, these values are higher than those previously suggested for the slip-rate (0.04-0.35 mm/yr; Martínez-Díaz et al., 2003; Masana et al., 2004).

ults in the area relative to stations located W from the AMF and E of the Palomares fault suggest even higher velocities (Echeverria et al., 2014). Thus, all evidence suggests that these slip rates are minimum values.

"Dust" events as paleoearthquakes

Earthquake shaking triggers rock falls, and these generate "dust" over large areas. This phenomenon has been described from recent earthquakes, such as the 2010 M7.2 El Mayor-Cucapah earthquake in Baja California, Mexico) (Fletcher et al., 2014) or in the 2011 Lorca earthquake (oral communications of neighbors and videos published in the web). Following these observations, and based on the data obtained at the new El Saltador trenches, we suggest here that some earthquakes may produce a clear signal in the stratigraphical record if these fine sediments, spread along large areas, are finally drained and concentrated in erosive channels and mostly preserved in narrow areas adjacent to a fault scarp that blocks the drainage (Masana et al., 2014). The

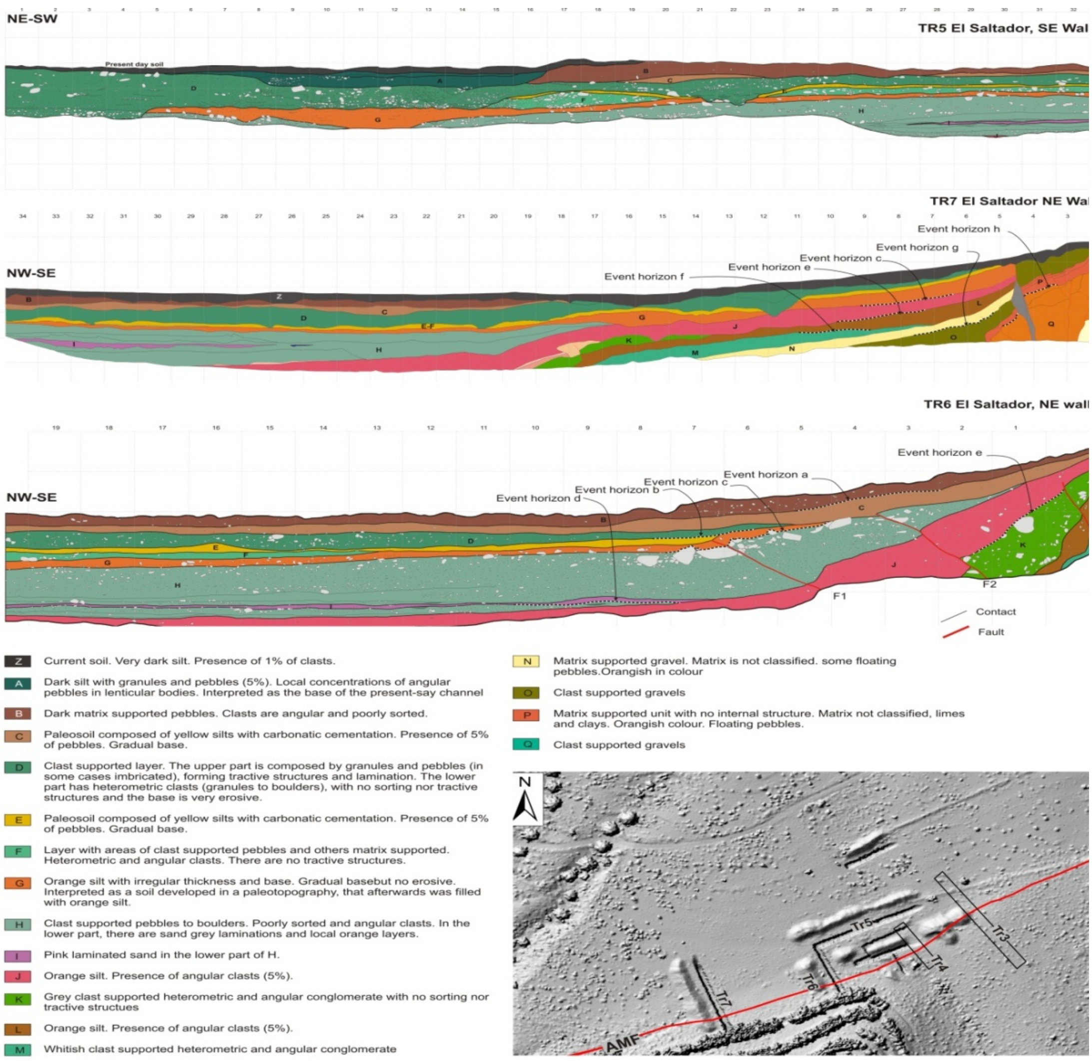

Fig 10.3. From top to bottom: logs of trenches 5, 7 and 6. Legend on the lower left. In the lower right corner, location map of the trenches at the Alhama de Murcia Fault trace

stratigraphy revealed by the trenches at El Saltador is mainly composed of coarse alluvial gravel strata (Figure 10.3, units B, D, F, H…) separated by periods of non-deposition and development of soils (Figure 10.32, units C or E). Pebbles or cobbles within these units are composed of philite and some limestone, eroded from La Tercia range strata.

This monotonous sequence is interrupted in the trenches by oxidized, fine-grained units (figure 5, units G, J, L, N, P) composed of silt and clay that contain some floating pebbles. These strata probably originated as mud flows that used preexisting erosive channels to flow from la Tercia range towards the Guadalentin depression (trench 5 shows how unit G is filling the lower parts of a paleochannel).

Trenches 6 and 7 were dug orthogonal to the fault. They show two types of deformational structures: a) faults located on its southeastern side and b) attenuated folds deforming strata up to unit E. Deformation in both cases is larger for older units than for younger ones, probably exhibiting evidence for the reverse slip component of the fault. Trench 5, being parallel to the fault, reveals the geometry of the silty units by showing how unit G behaves laterally.

We propose here that the fine grained units interpreted as mud flows are post-earthquake deposits and are linked genetically to the earthquakes themselves. The lines of evidence for this interpretation are the following:

a) Lithological. While the composition (clasts and matrix) of the units composing the alluvial fans in the area and in the trenches, mainly gravels, are easily correlatable with the composition of the units outcropping in the source area at La Tercia range, no correlation was found between these fine-grained oxidized units and the lithology in the source area: fine grained units with orangishcolour are lacking in La Tercia range. Not even the regionally present Miocene marls, that could be a source of fine grained sediments, crop out in the source area (and are, otherwise, grey-yellowish in color).

b) Geometry and distribution. The fine grained units show a channelized base and a tabular upper contact, change abruptly in thickness at the fault line and are usually absent on the uplifted wall of the fault, suggesting that the channelized mud flow followed and filled previous drainage scars on the morphological surface and that they were blocked by the co-seismic fault scarp, forming sporadic and localized mud-sheets. In this location, the fault uplifts the southeastern wall and, thus, dams the drainage towards the Guadalentin depression. Considering the low resistance to erosion of the gravels that would compose the fault scarp, the deposition of these units must have taken place soon after the earthquake (during the first large storm).

c) Stratigraphical. These fine grained units constitute an anomaly in the regional stratigraphy of the alluvial fans that are mainly composed of gravels interbedded locally with soils. How to explain such a sudden change of the source lithology in the drainage area? Soil formation in the source area could provide some oxidized fine sediments.However it would not explain why these units are recurrently interbedded in the sequence: why soils were not slowly eroded while they are being formed and instead formed thick units with sharp contacts with its upper and lower units? Uplifted wall could constitute a source of fines although the orangish sediments are cropping out far upstream and therefore this is unlikely.

Paleoearthquakes

According to this interpretation of the fine-grained units, trenches 6 and 7 can be interpreted to provide evidence of a minimum of eight paleoearthquakes. Figure 2 shows the horizon events we used for this interpretation.

Event a: The bottom of unit C is offset by F2 at trench 6 (vertical 4) while its contact with unit B is not offset. This implies that a deformation event (paleoearthquake) took place after the deposition of unit C or during its deposition. The event horizon could be placed also within unit C.

Event b: F1 is clearly deforming (folding) the bottom of unit G and its contact with unit E-F, while unit D is not folded. This suggests that an event different from event a took place after the deposition of unit E-F and before D.

Event c: Unit G was interpreted as a post-seismic dust concentration unit and therefore its base constitutes an event horizon.

Event d: Unit I is composed of fine, well sorted fine-grained sediment with internal lamination, but also with a part containing a large amount of lime and clay. This unit is not thus comparable with units G, J, L, N and P, as those do not show internal classification. However, the position of unit I, onlapping the deformation produced by F1 on the underlying deposits, and the high contents of lime, suggests a damming episode after the deformation of unit J. Such episodes are rare in the stratigraphic sequence and are therefore interpreted as an additional seismic event that modified the landscape, and dammed the stream draining towards the Guadalentin depression owing to the scarp uplift.

Events e, f, g and h: are based, in the same way as event c, on the presence of post-seismic dust concentration units J, L N and P, respectively.

In conclusion, we propose a new line of evidence for paleoearthquakes in this area that could be also described in other arid regions where earthquakes produce large amounts of dust due to rock falls. If correct, then there have been up to eight paleoearthquakes at El Saltador site, the longest earthquake sequence ever described along the Lorca-Totana segment of the fault. Further studies will focus on dating and correlating these events with lateral offsets, and thus to magnitude of paleoearthquakes, and will therefore allow us to better establish the seismic potential of the AMF

Acknowledgements: *This work has been funded by the Spanish research Projects SHAKE CGL2011-30005-C02-02 and supported by CSD2006-0004 "Topo-Iberia" (Consolider-Ingenio 2010).*

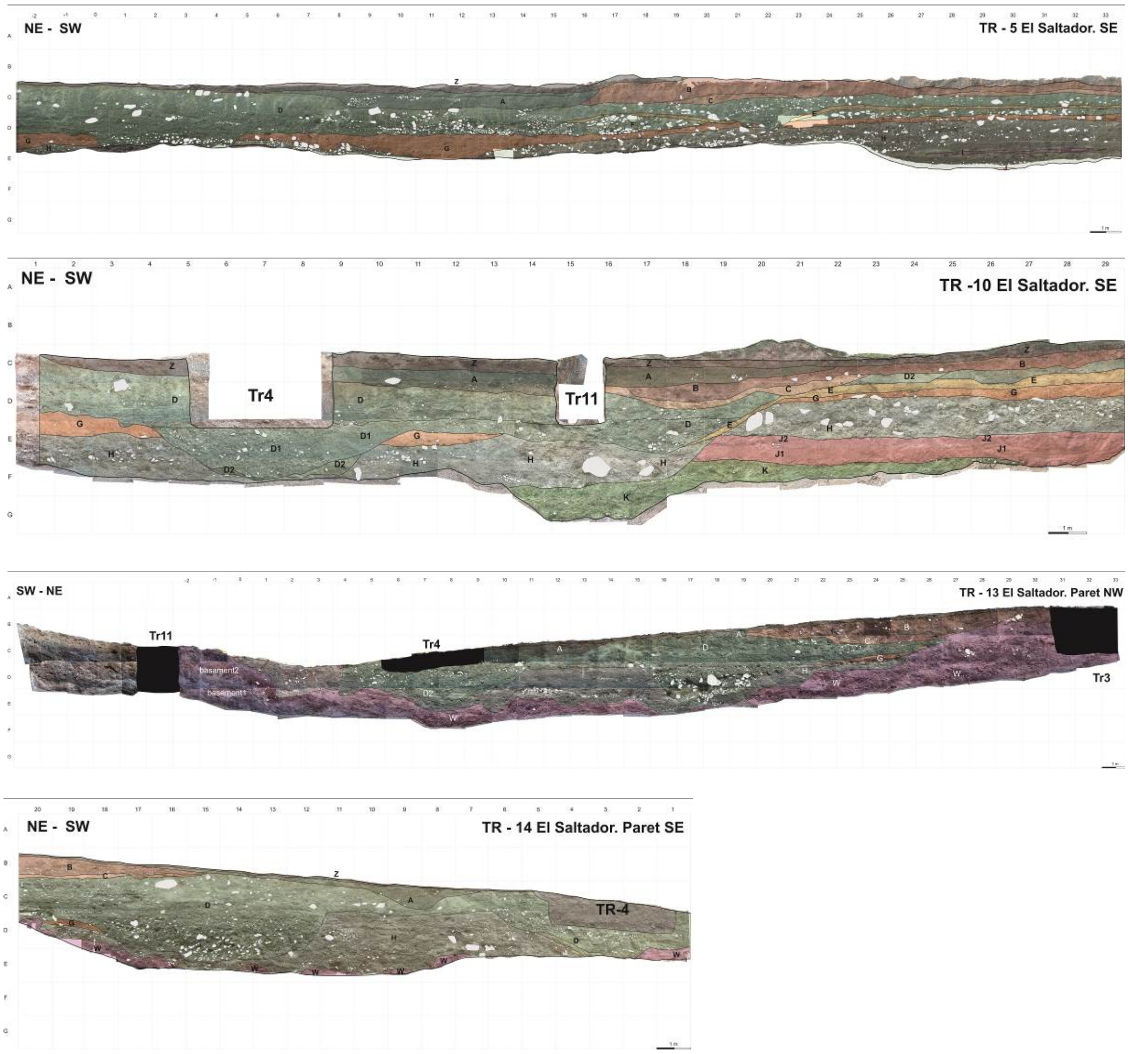

Fig. 10.4.Natural exposures of trenches 5, 10, 13 and 14 in El Saltador site Trenches used for the paleoearthquake characterization analysis

C³ References.

Alfaro P, Delgado J, García-Tortosa FJ, Lenti L, López JA, López-Casado C, Martino S (2011). Widespread landslides induced by the Mw 5.1 earthquake of 11 May 2011 in Lorca, SE Spain. *Engineering Geology* 137-138: 40-52.

Alfaro P, Bartolomé R, Borque J.M, Estévez A, García-Mayordomo J, García-Tortosa F.J, Gil A.J, Gràcia E, Lo Iacono C, Perea H (2012). The Bajo Segura Fault Zone: Active blind thrusting in the Eastern Betic Cordillera (SE Spain). *Journal of Iberian Geology* 38 (1), 271-284.

Alonso Zarza AM, Silva PG, Goy JL, Zazo C (1998). Fan-surface dynamics, plant-activity and calcrete development: Interactions during ultimate phases of fan evolution in the semiarid SE Spain (Murcia). *Geomorphology* 24: 147-167.

Bardají T (1999). *Evolución Geomorfológica durante el Cuaternario de las Cuencas Neógenas litorales del Sur de Murcia y Norte de Almería*. PhD Thesis, Universidad Complutense de Madrid, 492pp.

Bardají T, Civis J, Dabrio C., Goy JL, Somoza L, Zazo C (1986). Geomorfología y estratigrafía de las secuencias marinas y continentales cuaternarias de la Cuenca de Cope (Murcia, España). In: López, F., Thornes, J.B. (Eds.), *Estudios sobre Geomorfología del Sur de España*. Universidad de Murcia, 11–16.

Bardají, T., Goy, JL, Zazo, C, Hillaire-Marcel C, Dabrio CJ, Cabero A, Ghaleb B, Silva PG, Lario J (2009). Sea level and climate changes during OIS 5e in the Western Mediterranean. *Geomorphology* 104: 22–37.

Bardají T, Silva PG, Zazo C, Goy JL (2010). Cartografía y memoria del Cuaternario, Geomorfología y Procesoso Activos. Mapa Geológico Nacional, Serie MAGNA, 3ª Serie, IGME

Bardají T, Cabero A, Lario J, Zazo C, Silva PG, Goy JL, Dabrio CJ (2014). Coseismic vs climatic factors in the record of relative sea level changes: an example from the last interglacials in SE Spain. *Quaternary Science Reviews* (e.p.).

Calmel-Avila M (2000). Procesos hídricos holocenos en el Bajo Guadalentín (Murcia, España). Cuaternario y Geomorfología 14 (1-2): 65-78.

Calmel-Avila M (2002). The Librilla “rambla” anexample of morphogenetic crisis in theHolocene (Murcia, SE Spain). Quaternary International 93-94: 101-108.

Dabrio CJ, Zazo C, Goy JL, Santiesteban C, Bardaj| T, Somoza L, Baena J, Silva PG (1991). Neogene and Quaternary fan-delta deposits in southeastern Spain. Cuad. Geol. Iber. 15, 327-400.

De Prado C (1863). Los terremotos de la Provincia de Almería. *Revista Minera*, 14 (tomos 322 - 325), 180 pp.

Echeverria A, Khazaradze G, Asensio E, Gárate J, Martín-Dávila J, Suriñach E (2013). Crustal deformation in Eastern Betics from CuaTeNeo GPS network. *Tectonophysics*, 608: 600-612.

Espinar Moreno M (1994). Los terremotos históricos de la provincia de Almería. En: El estudio de los terremotos en Almería. Instituto de Estudios Almerienses, pp. 115-180.

Fernández Bolea E (2009). Los terremotos de 1863 en la comarca del Levante almeriense. *Espiral, Cuadernos del Profesorado*, 2 (3), 27-40.

Fletcher J. Rockwell T. Teran O, Hernandez AP, Mueller K, Owen L, Gold P, Elliott A, Akciz S, Sharp W, Gonzalez A, Spelz R (2014). 2013/2014 Friends of the Pleistocene field guide, 43 pp.

Ferrater M, Silva PG, Ortuño M, Rodríguez-Pascua MA, Massana E (2014). Análisis arqueosismológico del yacimiento de la Edad de Bronce de La Tira del Lienzo. *Resúmenes IBERFAULT II, Lorca.*

Ferrater M, Ortuño M, Masana E, Perea H, Baize S, Martínez-Díaz JJ, Pallàs R, García-Meléndez E, Echeverría A, Corominas, O, Rockwell T (2014a). Primeros valores de velocidad de deslizamiento lateral en la falla de Alhama de Murcia basados en trincheras 3D. *Resúmenes 2ª Reunión Ibérica sobre Fallas Activas y Paleosismología, IBERFAULT II*. Lorca, España. Octubre, 2014. pp. 19-22.

Ferrater M, Pallàs R, García-Meléndez E, Rockwell T, Sharp WD, Ortuño M, Masana E (2014b). Datación de carbonato pedogénico con la serie del U-Th. Aplicación en paleosismología: Datación de abanicos aluviales y de sucesión de unidades en el SE de la Península Ibérica. *Resúmenes 2ª Reunión Ibérica sobre Fallas Activas y Paleosismología, IBERFAULT II*. Lorca, España. Octubre, 2014. pp. 225-228.

Ferrater M, Silva PG, Ortuño M, Rodríguez-Pascua MA, Massana E (in press). Archaeoseismological analyis of a Late BronzeAgesiteonthe Alhama de Murcia Fault: La Tira del Lienzo (Totana). Geoarchaeology.

García Asensio E (1908). *Historia de la Villa de Huércal-Overa y su comarca precedida de un estudio físico-geológico de la cuenca del río Almanzora*. 295 pp.

Giménez J, Suriñach E, Goula X. (2000). Quantification of vertical movements in the eastern Betics (Spain) by comparing levelling data. *Tectonophysics* 317, 237-258.

Giner-Robles JL, Pérez-López R, Silva, PG, Rodríguez-Pascua MA, Martin-González F, Cabañas L (2012). Análisis estructural de danos orientados en el terremoto de Lorca del 11 de mayo de 2011: Aplicaciones en arqueosismologia. *Boletín Geológico y Minero* 123 (4). 503-513.

Harvey AM (1984). Debris flows and fluvial deposits in Spanish Quaternary alluvial fans: implications for fan morphology. *Canadian Soc Petrol Geol Mem* 10: 123-132.

Harvey AM (1990). Factors influencing Quaternary alluvial fan development in Southeast Spain. In: Rachocki AH, Church U (eds) *Alluvial Fans: a field approach*. John Willey & Sons, New York, USA.

IGN (1995). Sismicidad histórica del Reino de Granada (1487 – 1531). *Monografía Nº 12. IGN*, Madrid. 283 pp.

IGN (2014). Instituto Geográfico Nacional; Catálogo de terremotos [Online]. http://www.ign.es/

IGME (2011). *Informe geológico preliminar del Terremoto de Lorca del 11 de mayo de 2011 Mw 5.1*. IGME, Madrid (Spain). 47 pp.

Larouzière D, Bolze J, Bordet P, Hernández J, Montenat C, Ott D'Estevou P (1988). The Betic segment of the lithospheric Transalboran Shear Zone during the Late Miocene. *Tectonophysics* 152: 41-52.

López-Comino JA, Mancilla F, Morales J, Stich D (2012). Rupture directivity of the 2011, Mw 5.2 Lorca earthquake (Spain). *Geophys. Res. Lett.*, 39, L03301.

Madoz P (1845-50). *Diccionario Geográfico-Estadístico-Histórico de España y sus posesiones de Ultramar*. 16 Tomos, Madrid. http://www.diccionariomadoz.org/

Martínez-Díaz JJ (1998). *Geotectónica y tectónica activa del sector centro-occidental de la Región de Murcia y sur de Almería*. Tesis doctoral. Universidad Complutense de Madrid. 466 pp.

Martínez-Díaz JJ (2002). Stress field variation related to fault interaction in a reverse oblique-slip fault: the Alhama de Murcia fault, Betic Cordillera, Spain. *Tectonophysics* 356, 291–305.

Martínez-Díaz JJ, Masana E, Hernández-Enrile JL, Santanach P (2001). Evidence for coseismic events of recurrent prehistoric deformation along the

Alhama de Murcia fault, southeastern Spain. *Acta Geológica Hispánica*, 36 (3-4): 315-327.

Martínez-Díaz JJ, Masana E, Hernández-Enrile JL, Santanach P (2003). Effects of repeated paleo-earthquakes on the Alhama de Murcia fault (Betic Cordillera, Spain) on the Quaternary evolution of an alluvial fan system: *Annals of Geophysics*, 46, no. 5, p. 775–792.

Martínez-Díaz JJ, Álvarez-Gómez, J, García-Mayordomo J, Insua-Arévalo J, Martín-González F, Rodríguez-Peces MJ (2012). Interpretación tectónica de la fuente del terremoto de Lorca 2011 (Mw 5,2) y sus efectos superficiales. Boletín Geológico Minero, 123(4), 441-458.

Martínez-Díaz JJ, Masana E, Ortuño M. (2012) Active tectonics of the Alhama de Murcia fault, Betic Cordillera, Spain. *Journal of Iberian Geology* 38 (1): 170 -181

Martínez Solares JM., Mezcua J (2002). Catálogo Sísmico de la Península Ibérica (880 a.C. – 1900). *Monografías IGN* 18. IGN, Madrid (Spain), 253 pp.

Masana E, Martínez-Díaz JJ, Hernández-Enrile JL, Santanach P (2004). The Alhama de Murcia fault (SE Spain), a seismogenic fault in a diffuse plate boundary: Seismotectonic implications for the Ibero-Magrebian region: *Journal of Geophysical Research*, 109, 1–17

Masana E, Pallàs R, Perea H, Ortuño M, Martínez-Díaz JJ, García-Meléndez E, Santanach P (2005). Large Holocene morphogenic earthquakes along the Albox fault, Betic Cordillera, Spain. *Journal of Geodynamics* 40, 119–133.

Mezcua J (1982). *Catálogo General de Isosistas de la Península Ibérica*. Instituto Geográfico Nacional, Pub. 202, 319pp.

Michetti AM, Esposito E, Guerreri L, Porfido S, Serva L, Tatevosian R, Vittori E, Audemard F, Azuma T, Clague J, Comerci V, Gürpinar A, McCalpin J, Mohammadioun, B, Mörner N A, Ota Y, Roghozin E (2007) *Intensity Scale ESI 2007*. (Guerreri & Vitori Eds.) Memorie Descrittive della Carta Geologica d'Italia, vol. LXXIV, Servizio Geologico d'Italia, APAT, Rome.

Meijninger B (2006).*Late-orogenic extension and srike-slip deformation in the neogene of southeastern Spain*. Doctoral Thesis. Utrecht University.

Niemeijer AR, Vissers RL (2014). Earthquake rupture propagation inferred from the spatial distribution of fault rock frictional properties. *Earth and Planet. Sci. Lett.*, 396, 154-164.

Oliveros MA (1987). *Estudio tectónico-cinemático de la fracturación reciente en el borde oriental y suboriental de la Sierra de las Estancias (Murcia y Almería)*. Tesis de Licenciatura. Universidad Complutense de Madrid, 100 pp.

Oohashi K, Hirose T, Shimamoto, T (2013). Graphite as a lubricating agent in fault zones: An insight from low- to high-velocity friction experiments on a mixed graphite-quartz gouge. *Journal of geophysical research: Solid earth*, 118, 2067–2084.

Ortuño M, Masana E, García-Meléndez E, Martínez-Díaz JJ, Canora C, Štepancíková P, Cunha P, Sohbati R, Buylaert JP, Murray AS (2012). Paleoseismic study of a slow-moving and silent fault termination: the Alhama de Murcia-Góñar system (Eastern Betics, Spain). *Geological Society of America Bulletin*.

Rodríguez-Escudero E, Martínez-Díaz JJ, Tsige M (2012). Deformaciones pseudodúctiles en régimen frágil en una falla activa lenta: la Falla de Alhama de Murcia. Implicación sismotectónica. *GeoTemas*, 13, 1531-1534.

Rodríguez-Escudero E, Martínez-Díaz JJ, Tsige M, Giner-Robles JL, Cuevas-Rodríguez J (2014). Cuarzo pulverizado en la faultgouge rica en filosilicatos de la Falla de Alhama de Murcia: ¿Un efecto cosísmico? *Resúmenes de IBERFAULT II, Lorca.*

Rodríguez-Pascua MA, Pérez-López R, Giner-Robles JL, Silva PG, Garduño-Monroy VH, Reicherter K (2011). A comprehensive classification of earthquake archaeological effects (EAE) in archaeoseismology: application to ancient remains of roman and mesoamericon cultures. *Quaternary International* 242, 20-30.

Rodriguez-Pascua, MA, Perez-Lopez R, Martin-Gonzalez F, Giner-Robles JL, Silva PG (2012). Efectos arquitectónicos del terremoto de Lorca del 11 de mayo de 2011. Neoformacion y reactivación de efectos en el Patrimonio Cultural. *Boletín Geológico y Minero* 123 (4). 487-502.

Rutter EH, Maddock RH, Hall SH, White S (1986). Comparative microstructures of natural and experimentally produced clay-bearing fault gouges. *Pageophysics*. 124 (1-2): 3-30.

Shobati R, Murray AS, Buylaert JP, Ortuño M, Cunha P, Masana E (2011). Luminescence dating of Pleistocene alluvial sediments affected by the Alhama de Murcia fault (eastern Betics, Spain) – a comparison between OSL, IRSL and post-IR IRSL ages. *Boreas* 10, 2-13.

Silva PG (1994). *Evolución Geodinámica de la Depresión del Guadalentín desde el Mioceno Superior hasta la actualidad: Neotectónica y Geomorfología*. Ph.D. UCM, Madrid, Spain. 642pp.

Silva PG (1996). Geometría fractal de la Falla de Lorca-Alhama de Murcia (SE España). *Geogaceta* 20(6). 1385-1389.

Silva PG (2014).The Guadalentín Tectonic Depression (Betic Cordillera, Murcia). In: *Landscapes and Landforms of Spain* (F. Gutiérrez and M. Gutiérrez Eds). World Geomorphological Landscapes Series. Springer Science. Dordrecht, Germany. pp. 25 - 35

Silva PG, Goy JL, Zazo C (1992a) Características estructurales y geométricas de la Zona de Falla de Lorca-Alhama. *Geogaceta* 12: 7-11.

Silva PG, Harvey AM, Zazo, C, Goy, JL (1992b) Geomorphology, depositional style and morphometric relationships of Quaternary alluvial fans in the Guadalentin Depression (Murcia, SE Spain). *Z F Geomorphologie* 36: 661-673.

Silva PG, Goy JL, Somoza L, Zazo C, Bardají T (1993) Landscape response to strike-slip faulting linked to collisional settings: Quaternary tectonics and basin formation in the Eastern Betics, Southeast Spain. Tectonophysics 224: 289-303.

Silva PG, Goy JL, Zazo C, Bardají T (1996) Evolución reciente del drenaje en la Depresión del Guadalentín (Murcia). *Geogaceta* 20(6): 1385-1389.

Silva PG, Goy JL, Zazo C, Lario J. Bardají T (1997) Palaeoseismic indications along "aseismic" fault segments in the Guadalentín Depression (SE Spain). *J. Geodynamics* 24: 105-115.

Silva PG, Goy JL, Zazo C, Bardají T (2003) Fault generated mountain fronts in southeast Spain: geomorphologic assessment of tectonic and seismic activity. *Geomorphology* 250: 203-226.

Silva PG, Calmel-Avila M, Bardají T, Goy JL, Zazo C (2008) Transition from alluvial to fluvial systems in the Guadalentin Depression (SE Spain) during the Holocene: Lorca Fan versus Guadalentín River. Geomorphology 100: 144-153.

Silva P G, Pérez-López R, Rodríguez-Pascua M A, Roquero E, Giner J L., Huerta P, Bardají T (2014). Macroseismic analysis of slope movements triggered by the 2011 Lorca Earthquake (Mw 5.2): Application of the ESI-07 scale. *Geogaceta*, 55. (en prensa).

Silva PG, Rodríguez-Pascua MA., Giner-Robles JL, Roquero E, Pérez-López R, Huerta P, Bardají T

(2014). Anatomy of an Earthquake: Geological analysis of the Huércal-Overa AD 1863 event (Almería, SE Spain). *Resúmenes 2ª Reunión Ibérica sobre Fallas Activas y Paleosismología, IBERFAULT II*. Lorca, España. Octubre, 2014.

Stokes M, Mather AE (2003). Tectonic origin and evolution of a transverse drainage: the Rio Almanzora, Betic Cordillera, Southeast Spain. *Geomorphology* 50, 59–81.

Zazo C, Goy JL, Dabrio CJ, Lario J, González-Delgado A, Bardají T, Hillaire-Marcel C, Cabero A, Ghaleb B, Borja F, Silva PG, Roquero E, Soler V (2013). Retracing the Quaternary history of sea-level changes in the Spanish Mediterranean-Atlantic coasts: Geomorphological and sedimentological approach. *Geomorphology* 196, 36-49.

C³ Cuadernos de Campo del Cuaternario Vol., 1. 2014. AEQUA, Madrid. 36 pp.

Silva P G, Bardají T, Rodríguez-Pascua A M, Roquero E, Martínez Díaz, JJ, Eds. (2014). *Tectonic Geomorphology and paleoseismic records in the Eastern Betic Shear Zone and Aguilas Arc (Murcia - Almería, SE Spain).*